Excitation of Plasma Waves by Gaps and Slow-Wave Structures[+)]

H. Derfler

IPP IV/77 September 1974

MAX-PLANCK-INSTITUT FÜR PLASMAPHYSIK

GARCHING BEI MÜNCHEN

MAX-PLANCK-INSTITUT FÜR PLASMAPHYSIK

GARCHING BEI MÜNCHEN

Excitation of Plasma Waves by Gaps and Slow-Wave Structures[+)]

H. Derfler

IPP IV/77 September 1974

+) invited paper presented at the International School of Plasma Physics Symposium on "Plasma Heating in Toroidal Devices", Varenna, Italy, 3 - 17 September 1974

Die nachstehende Arbeit wurde im Rahmen des Vertrages zwischen dem Max-Planck-Institut für Plasmaphysik und der Europäischen Atomgemeinschaft über die Zusammenarbeit auf dem Gebiete der Plasmaphysik durchgeführt.

IPP IV/77 H. Derfler

Excitation of Plasma Waves by Gaps and Slow-Wave Structures[+)]

September 1974 (in English)

Abstract

Maxwell's equations are solved for a cylindrical waveguide containing a magneto plasma with a prescribed dentity profile. A complete set of orthogonal azimutal and radial modes, and their dispersion relations is obtained. Power flux and surface current are then used to define a power-equivalent R.F. plasma potential and a characteristic wave impedance for each mode. The result is applied to axisymmetric systems of plasma wave excitation consisting of a sequency of gaps in the waveguide, connected to circuits of any kind. The respective boundary value problems are reduced to the case of a single gap with surface currents and power equivalent plasma potentials prescribed at two locations left and right from the gap. The Green's function is obtained for that case and used to set up an integral equation for the electric field along a surface bounded by the gap. An approximate solution based on Schwinger's variational principle amounts to matching the admittances looking both ways through the gap. That gives three by three admittance matrices, one for each mode, which relate the surface currents and potentials at the prescribed locations and at the gap. These mode-equivalent T-junctions are then used in conjunction with Floquet's theorem to synthesize the system of a periodic array of gaps connected to an iterated circuit. The re-

sulting coupled mode equation for Floquet's propagation constant shows that efficient transfer of power from the circuit to the plasma wave requires a close match of their phase velocities, and - for broad band operation - also a close match of their group velocities. These criteria lead to the design of a slow-wave directional coupler, which is applicable in the appropriate frequency regions. Sample calculations show that these requirements are met by plasma waves in a frequency range between the lower-hybrid frequency and the electron plasma frequency.

+) invited paper presented at the
International School of Plasma Physics Symposium on
"Plasma Heating in Toroidal Devices", Varenna, Italy,
3 - 17 September 1974

1. Introduction

The theory of plasma wave excitation has found little attention so far in the community of plasma physicists, although this problem is of prime importance in R.F. plasma heating. A fameous exception represents the excellent work of T.H. Stix[1] on the excitation of Alfvèn- and ion-cyclotron waves by means of coils of finite size. One can make an extensive search through the literature on plasma physics before one can find such tangible results as coil-impedance and plasma-loading, which are the basis for any engineering design procedures. The author's[2] own work in this field was largely restricted to the case of plane parallel grids in an infinitly extended plasma. Since internal structures of a fragile nature cannot be tolerated in fusion devices, alternative coupling schemes must be found. The literature on microwave-high-power devices offers a formidable source of ideas in that respect, along with powerful analytical techniques to predict the performance of such devices. It is quite amazing that little, if any, effort has been made so far by plasma physicists to tap these resources. A step in that direction must be taken eventually, at the latest when we have to exactly specify our requirements for plasma heating to the manufacturer of high-power R.F. equipment. In this paper we take two such steps. The first by analyzing a basic coupling scheme which does not require any parts suspended inside the plasma container, the second by presenting the performance data in conventional engineering terms. The latter is made possible by the methode of analysis, which represents a sophisticated extension of the early work by the author [3,4,5,6] on high-power microwave tube devices, here applied to basic plasma physics.

The system analyzed in this paper consists of a cylindrical waveguide, filled with a magneto plasma whose dielectric tensor elements $\varepsilon_{\parallel}$, ε_{x}, $\varepsilon_{\perp}$ can be specified along with any radial density profile. In order to arrive at differential equations rather than integral equations, compare e.g. H. Derfler and F. Leuterer [7], we use here the cold plasma approximation though the effects of parallel temperature can be included without essential difficulties. After Fourier analysis in axial direction we

obtain in chapter 2 the complete set of azimutal and radial modes, and show that the inter-mode Poynting flux is quasi diagonal in the presence of small losses. Power flux and surface current are used to define a R.F.-potential and a characteristic wave impedance for each mode. Together with the dispersion characteristics we thus obtain a set of mode-equivalent transmission lines of standard engineering type. The phenomenon of non-reciprocal propagation is then excluded from this paper by restricting the subsequent considerations to devices with azimutal symmetry. In chapter 3 we consider a single gap in the waveguide connected to a radial transmission line. To solve the inhomogeneous boundary conditions we first generate a Green's function by Fourier analyzing the electric field along the wall and subsequent residue calculation. An application of Schwinger's [8] variational principle then allows to match the admittances looking both ways through the gap, using a trial function for the axial electric field in the gap. The resulting normal mode expansion contains amplitude factors whose square is equal to the fraction of power fed into each mode. Expressions are then obtained for the load impedance of the gap and the losses in the wall. In chapter 4 we first generalize this system by specifying surface currents at two locations left and right of the gap. To match the boundary conditions at these "virtual terminals" we simply add a spectrum of standing waves to the amplitude factors of chapter 2. That gives 3 x 3 "admittance matrices", one for each mode, which determine the surface currents and potentials at the virtual terminals as a function of these at the gap-input terminals. These mode-equivalent T-junctions are then used in conjunction with Floquet's theorem to synthesize the system of a periodic array of gaps connected to a space-periodic circuit. The resulting dispersion relation for Floquet's propagation constant shows both, forward and backward wave interaction between circuit and plasma waves. A one to one correspondence is then established with the conventional microwave theory of directional couplers, from which we can quote directly the properties a slow wave directional coupler must have for the purposes of R.F. plasma heating.

2. Normal Modes and Transmission-Line Analogue

When Maxwell's equations for a cylindrical magnetoplasma

$$\nabla \times \vec{H} = j\omega \epsilon_0 \underline{\underline{\epsilon}} \cdot \vec{E} \qquad \nabla \times \vec{E} = -j\omega \mu_0 \vec{H} \qquad \underline{\underline{\epsilon}} = \begin{bmatrix} \epsilon_\perp & j\epsilon_x & 0 \\ -j\epsilon_x & \epsilon_\perp & 0 \\ 0 & 0 & \epsilon_\parallel \end{bmatrix} \tag{1}$$

are Fourier analyzed in the form

$$E_\gamma(r,\phi,z) = \frac{1}{4\pi^2} \sum_{m=-\infty}^{+\infty} \int_{-\infty}^{+\infty} dk \; \hat{E}_{\gamma m}(r,k)\, e^{-jm\phi - jkz} \qquad \gamma = r,\varphi,z \tag{2}$$

one can eliminate the radial fields

$$\begin{aligned} \hat{E}_{rm} &= \left(k\hat{H}_{\phi m} - \frac{m}{r}\hat{H}_{zm} - j\omega\epsilon_0\epsilon_x \hat{E}_{\phi m} \right) / \omega\epsilon_0\epsilon_\perp \\ \hat{H}_{rm} &= \left(-k\hat{E}_{\phi m} + \frac{m}{r}\hat{E}_{zm} \right) / \omega\mu_0 \end{aligned} \tag{3}$$

and obtains the following system of first order differential equations describing the radial evolution of the Fourier components:

$$\frac{d}{d\rho} \begin{bmatrix} \hat{E}_{zm} \\ \frac{j}{K}\sqrt{\frac{\mu_0}{\epsilon_0}}\hat{H}_{zm} \\ -\frac{\rho}{K}\hat{E}_{\phi m} \\ -j\rho\sqrt{\frac{\mu_0}{\epsilon_0}}\hat{H}_{\phi m} \end{bmatrix} = \frac{1}{\rho} \begin{bmatrix} 0 & \frac{m}{\epsilon_\perp}K^2 & \frac{\epsilon_x}{\epsilon_\perp}K^2 & \frac{1}{\epsilon_\perp}K^2 - 1 \\ m & m\frac{\epsilon_x}{\epsilon_\perp} & K^2 - \frac{\epsilon_\perp^2 - \epsilon_x^2}{\epsilon_\perp} & \frac{\epsilon_x}{\epsilon_\perp} \\ 0 & \rho^2 - \frac{m^2}{\epsilon_\perp} & -m\frac{\epsilon_x}{\epsilon_\perp} & -\frac{m}{\epsilon_\perp} \\ \epsilon_\parallel\rho^2 - m^2 & 0 & -mK^2 & 0 \end{bmatrix} \cdot \begin{bmatrix} \hat{E}_{zm} \\ \frac{j}{K}\sqrt{\frac{\mu_0}{\epsilon_0}}\hat{H}_{zm} \\ -\frac{\rho}{K}\hat{E}_{\phi m} \\ -j\rho\sqrt{\frac{\mu_0}{\epsilon_0}}\hat{H}_{\phi m} \end{bmatrix} \tag{4}$$

Here $\rho \equiv r\omega/c$, and $K \equiv ck/\omega$ the refractive index parallel to the applied magnetic field. This system has the form of Birkhoff and Langer [9],

$$\frac{d}{d\rho}\,\underline{X}_m = \left(\underline{\underline{A}}_m + \lambda\,\underline{\underline{B}}_m\right)\cdot\underline{X}_m \qquad (5.1)$$

with eigenvalue $\lambda = K^2$, and boundary conditions

$$X_{1m}(\alpha) = X_{3m}(\alpha) = 0\,, \quad \lim_{\rho\to 0}\ \rho X_{2m}(\rho) = \rho X_{4m}(\rho) = 0 \qquad (5.2)$$

at the metal wall, $\alpha \equiv a\omega/c$, and in the center of the plasma respectivly. The latter condition excludes the two basic solutions of Eq.(5.1) which one can show to be singular at the origin $\rho = o$. The remaining two basic solutions serve to match the boundary conditions as follows. Using a trial value of λ, we start off computation at the origin $\rho = o$ with Taylor expansions

$$\underline{X}_m^{(i)}(\lambda,\rho) = \rho^m\left[\underline{C}_m^{(i)} + \rho^2\,\underline{D}_m^{(i)} + \ldots\right], \quad \underline{\tilde{C}}_m^{(1)}\cdot\underline{C}_m^{(2)} = 0,$$

then continue with a standard procedure for solving first order systems of differential equations, such as Hamming's. Simultaneously we calculate the determinant

$$\Delta_m(\lambda,\rho) \equiv \begin{Vmatrix} X_{1m}^{(1)}(\lambda,\rho) & X_{1m}^{(2)}(\lambda,\rho) \\ X_{3m}^{(1)}(\lambda,\rho) & X_{3m}^{(2)}(\lambda,\rho) \end{Vmatrix} \qquad (6)$$

and check if $\Delta_m(\lambda,\alpha) = o$? If not, a better trial value λ is predicted and the process is repeated until $\Delta_m(\lambda,\alpha) = o$ comes true. The resulting $\lambda = \lambda_{mn}$ is an eigenvalue and the corresponding eigenfunction $\underline{X}_{mn}(\rho)$ is a simple linear combination of the two basic solutions

$$X_{\gamma m}(\lambda,\rho) \equiv \begin{Vmatrix} X_{\gamma m}^{(1)}(\lambda,\rho) & X_{\gamma m}^{(2)}(\lambda,\rho) \\ X_{3m}^{(1)}(\lambda,\alpha) & X_{3m}^{(2)}(\lambda,\alpha) \end{Vmatrix}, \quad \gamma = 1\to 4\,, \qquad (7.1)$$

namely

$$\underline{X}_{mn}(\rho) \equiv \underline{X}_{m}(\lambda_{mn}, \rho) \tag{7.2}$$

As an example we show in Fig.1 the dispersion characteristic,

$$k_{m,n}(\omega) = \frac{\omega}{c}\sqrt{\lambda_{mn}(\omega)} \tag{7.3}$$

obtained for m = o radial modes of electromagnetic waves in a cylindrical waveguide filled with a cold magneto plasma with a Gaussian density profile. In the electrostatic limit, these waves are known as Trievelpiece Gould waves[10]. It is seen that phase and group velocity become slower the more radial nodes of oscillations, n, fit into the plasma. This agrees with Birkhoff and Langers[9] general statement that $|\lambda_{mn}| < |\lambda_{mn+1}|$. Since the matrices $\underline{\underline{A}}_m$ and $\underline{\underline{B}}_m$ in Eq.(4) are non hermitian, the eigenvalues λ_{mn} can be positive or negative in a loss-free plasma, corresponding to propagating waves (k_{mn} = real) or evanescent waves (k_{mn} = imaginary) respectively. When losses are introduced ($\varepsilon_\perp$, ε_x, $\varepsilon_\parallel$ complex) or when the frequency ω is taken to be complex as in Laplace analysis, $\underline{\underline{A}}_m$ and $\underline{\underline{B}}_m$ become complex, giving complex eigenvalues. Yet, the corresponding eigenfunctions are orthogonal. This can be shown from the adjoint system of equations:

$$\frac{d}{d\rho}\underline{\tilde{Y}}_m^* = -\underline{\tilde{Y}}_m^* \cdot \left(\underline{\underline{A}}_m + \lambda \underline{\underline{B}}_m\right) \tag{8.1}$$

with boundary conditions

$$Y_{2m}(\alpha) = Y_{4m}(\alpha) = 0, \quad \lim_{\rho\to 0} \rho Y_{1m}(\rho) = \rho Y_{3m}(\rho) = 0, \tag{8.2}$$

and from Green's identity which follows from

$$\frac{d}{d\rho}\underline{\tilde{Y}}_{mn}^* \cdot \underline{X}_m = \left(\frac{d}{d\rho}\underline{\tilde{Y}}_{mn}^*\right)\cdot \underline{X}_m + \underline{\tilde{Y}}_{mn}^* \cdot \left(\frac{d}{d\rho}\underline{X}_m\right) =$$

$$= (\lambda - \lambda_{mn})\, \underline{\tilde{Y}}_{mn}^* \cdot \underline{\underline{B}}_m \cdot \underline{X}_m .$$

by integration:

$$Y^{*}_{lmn}(\alpha)\, X_{lm}(\lambda,\alpha) = (\lambda-\lambda_{mn}) \int_0^{\alpha} \underline{\tilde{y}}^{*}_{mn} \cdot \underline{\underline{B}}_m \cdot \underline{X}_m \, d\rho \qquad (9.1)$$

In the last step we have taken the boundary conditions Eqs.(8.2) for Y_{mn} into account. Following Langer[11], the adjoint system Eqs.(8) has the same eigenvalues λ_{mn} as the original system Eqs. (5). Thus, if $\lambda = \lambda_{mp}$ is one such eigenvalue with eigenfunction $X_{mp}(\rho)$, the left-hand-side of Eq.(9) vanishes by virtue of the boundary conditions Eq.(5.2), which proofs the stated orthogonality:

$$\int_0^{\alpha} \underline{\tilde{y}}^{*}_{mn} \cdot \underline{\underline{B}}_m \cdot \underline{X}_{mp} \, d\rho = 0 \,, \quad n \neq p \qquad (9.2)$$

The case n = p can be obtained in the limit $\lambda \to \lambda_{mn}$, using Taylor expansion with respect to λ

$$Y^{*}_{lmn}(\alpha)\, X_{lm,\lambda n}(\alpha) = \int_0^{\alpha} \underline{\tilde{y}}^{*}_{mn} \cdot \underline{\underline{B}}_m \cdot \underline{X}_{mn} \, d\rho \,, \qquad (9.3)$$

where we have used the conventional subscript-comma notation to indicate partial derivative with respect to λ:

$$X_{lm,\lambda n}(\alpha) \equiv \left[\frac{\partial}{\partial\lambda} X_{lm}(\lambda,\alpha)\right]_{\lambda=\lambda_{mn}} = \Delta_{m,\lambda}(\alpha)\Big|_{\lambda=\lambda_{mn}}$$

This derivative is easily computed along with the basic solutions due to the fact that $X_m(\lambda,\alpha) = \Delta_m(\lambda,\alpha)$, and serves in the normalization of the eigenfunctions as described further below. Also, there is no need to solve the adjoint system eqs.(8) explicitly, because one can show by substitution, that it is equivalent to the original system under the transformation

$$\underline{Y}^* = \underline{\underline{T}} \cdot \underline{X} \quad , \quad \underline{\underline{T}} = \begin{pmatrix} 0 & 0 & 0 & 1 \\ 0 & 0 & \lambda & 0 \\ 0 & -\lambda & 0 & 0 \\ -1 & 0 & 0 & 0 \end{pmatrix} \tag{9.4}$$

By means of this transformation we can write Eqs. (9.2) and (9.3) in the common form,

$$\int_0^{\alpha} \underline{\tilde{R}}_{mn}(\rho) \cdot \underline{\underline{\tilde{T}}}_{mn} \cdot \underline{\underline{B}}_m(\rho) \cdot \underline{R}_{mp}(\rho)\, d\rho = \delta_{np}, \tag{9.5}$$

where

$$\underline{R}_{mn}(\rho) = \underline{X}_{mn}(\rho) \left[X_{4mn}(\alpha) X_{1m,\lambda n}(\alpha) \right]^{-1/2} \tag{9.6}$$

are the normalized eigenfunctions.

We now calculate the "mixed" Poynting flux in positive z-direction, which in view of Eq. (9.6) can be expressed in the form

$$2P_{mnp} = 2\pi \int_0^{\alpha} \left[\hat{E}_{rmp} \hat{H}^*_{\phi mn} - \hat{E}_{\phi mp} \hat{H}^*_{rmn} \right] r\, dr =$$

$$\left(\frac{c}{\omega}\right)^2 2\pi \sqrt{\frac{\epsilon_0}{\mu_0}}\, K_{mp} \left[X^*_{4mn}(\alpha) X^*_{1m,\lambda n}(\alpha) X_{4mp}(\alpha) X_{1m,\lambda p}(\alpha) \right]^{1/2} \int_0^{\alpha} S_{mnp}(\rho)\, d\rho , \tag{10.1}$$

where

$$S_{mnp} \equiv \frac{1}{\rho} \left[\frac{1}{\epsilon_\perp} \left(m R_{2mp}(\rho) + \epsilon_x R_{3mp}(\rho) + R_{4mp}(\rho) \right) R^*_{4mn}(\rho) + \left(m R_{1mn}(\rho) + \lambda_{mn} R_{3mn}(\rho) \right)^* R_{3mp}(\rho) \right]$$

$$= \underline{\tilde{R}}^*_{mn}(\rho) \cdot \underline{\underline{\tilde{T}}}^*_{mn} \cdot \underline{\underline{B}}_m(\rho) \cdot \underline{R}_{mp}(\rho) \tag{10.2}$$

Comparison with Eq. (9.5) shows, that due to the conjugate complex quantities indicated by the superscript star, the off diagonal elements $n \neq p$ of Eq. (10.1) do not vanish, except in the absence of losses where all is real in Eq. (10.2). The latter is true even in the presence of evanescent waves, because only the real quantity $K_{mn}^2 = \lambda_{mn} < 0$ is involved in that case. Our example shows that,

contrary to popular believe, the orthogonality of eigenfunctions and the diagonality of the mixed Poynting flux are two entirely different things. However, when the losses are small, $\nu_{coll}/\omega \ll 1$, one can show from Eqs.(9.5) that for $m \neq p$:

$$\left| \text{Real} \int_0^{\alpha} d\varrho \, S_{mnp} \right] \approx (\nu_{coll}/\omega)^2 \lll 1$$

and therefore we can neglect for all practical purposes the exchange of power between different modes. Thus we write for future reference the approximate "orthogonality condition"

$$\int_0^{\alpha} S_{mnp}(\varrho)\, d\varrho = \int_0^{\alpha} \underline{\tilde{R}}^{*}_{mn}(\varrho) \cdot \underline{\underline{\tilde{T}}}^{*}_{mn} \cdot \underline{\underline{B}}_{m}(\varrho)\, \underline{R}_{mp}(\varrho)\, d\varrho \approx \delta_{np} \qquad (10.3)$$

and

$$2 P_{mnp} = 2\pi \sqrt{\frac{\epsilon_0}{\mu_0}} \left(\frac{c}{\omega}\right)^2 K_{mn} \left| X_{4mn}(\alpha)\, X_{1m,\lambda n}(\alpha) \right| \delta_{np} \quad . \qquad (10.4)$$

This result is related in a simple way to the important engineering concept of wave impedance Z_{mn}, if we request that

$$2 P_{mnp} \equiv e_{mp}\, i^{*}_{mn} = i_{mn}\, i^{*}_{mn}\, Z_{mn}\, \delta_{np} \,, \qquad (11.1)$$

where

$$i_{mn} = -2\pi a \hat{H}_{\phi mn}(a) = \frac{2\pi c}{j\omega} \sqrt{\frac{\epsilon_0}{\mu_0}}\, X_{4mn}(\alpha) \qquad (11.2)$$

is the mean z-directed surface current, and $e_{mn} = i_{mn}\, Z_{mn}$, the voltage across a mode-equivalent transmission line with matched termination. Equating the expressions Eq.(10.4) and Eq.(11.1) then gives the simple formula

$$Z_{mn} = \frac{1}{2\pi} \sqrt{\frac{\mu_0}{\epsilon_0}}\, K_{mn} \left| R_{4mn}(\alpha) \right|^{-2} \qquad (11.3)$$

for the wave impedance. We also note for future reference that the ratio

$$Z_{mn} / K_{mn} = Z_{mn}^{*} / K_{mn}^{*} \qquad (11.4)$$

is strictly real.

In Fig.2 we show the result of a sample calculation representing the mode impedance Z_{on} for the electromagnetic Trievelpiece-Gould waves of Fig.1. The frequency range corresponds to the limited range in which we have been interested so far. To get an overview of how the wave impedance varies in a wider frequency range we also show in Fig.3 the analytic result

$$Z_{on} = \frac{1}{4\pi} \sqrt{\frac{\mu_o}{\epsilon_o}} \left(\frac{\omega_p^2 + \omega_n^2 - \omega^2}{\omega_p^2 - \omega^2} \right)^{1/2}$$

obtained for electromagnetic Trievelpiece-Gould waves in a pipe filled with homogeneous plasma at infinite magnetic field. This graph clearly shows the characteristics of a band-rejection filter, with cut-off frequencies at the plasma frequency ω_{pe} and hybrid frequency, $\omega_{nH} \equiv (\omega_p^2 + \omega_n^2)^{1/2}$, determined by the cut-off frequencies $\omega_n = p_n\, c/a$, $J_o(p_n) = o$, of the empty pipe. It is the lower pass-band, well above the lower hybrid frequency, which is of major interest to us in plasma heating. Both figures show that the wave impedances are in a convenient engineering range. Nevertheless deviations from it will occur in the load impedances of the couplers, say at two locations along the plasma. The effects due to the interference of incident and reflected waves of one particular mode are then accurately described by the standard transmission line equation:

$$\begin{bmatrix} i_{mn}^{(1)} \\ i_{mn}^{(2)} \end{bmatrix} = \frac{1}{jZ_{mn}} \begin{bmatrix} \cot g\, \ell k_{mn} & -\operatorname{cosec} \ell k_{mn} \\ -\operatorname{cosec} \ell k_{mn} & \cot g\, \ell k_{mn} \end{bmatrix} \cdot \begin{bmatrix} e_{mn}^{(1)} \\ e_{mn}^{(2)} \end{bmatrix} \qquad (12)$$

where $i_{mn}^{(i)}$ are the surface currents, and $e_{mn}^{(i)}$ the corresponding voltages at these locations i = 1, 2, spaced a distance 1 apart. The symmetry of the admittance matrix, $Y_{mn}^{(ik)} = Y_{mn}^{(ki)}$, in Eq.(13) shows that the propagation of each mode is reciprocal, though the mangeto plasma is known to be an optically active medium. As pointed out by H. Gamo[12], who treated the dual case of ferrite-loaded waveguides, one needs two modes, $\exp(\mp jm\phi - j z k_{\pm mn})$, to obtain polarization; with Faraday rotation due to $k_{mn}(\omega) \neq k_{-mn}(\omega)$. Both ingredients are needed in order to build a non-reciprocal device such as a unidirectional coupler. Though non-reciprocal propagation can have most important applications in R.F.-plasma heating, we defer the treatment of this subject to a future publication.

In the following sections we will be concerned exclusively with devices designed to excite azimutally symmetric modes, m = o. All we need in this task are the mode impedance, $Z_{on}(\omega)$, and the dispersion functions, $k_{on}(\omega)$, obtained in this section. We therefore shall suppress hence forth the subscript m = o, with the understanding that the remaining subscript, n, counts the radial nodes of oscillation in the plasma.

3. Gap Excitation of Plasma Waves

Consider a magneto-plasma contained in a metal pipe with a slit, and a radial transmission line connected to it, as shown in Fig.4. When a TM_o-wave is lounged by the generator connected to the radial transmission line, we have $E_\phi(z,r) = o$ for $r \geqq a$. Then any distribution of the axial field in the gap, $E_z(a,z) \equiv E(z)$, uniquely determines the other components of the electromagnetic field throughout the plasma and the radial transmission line. However, there is only one correct distribution of $E(z)$ which allows to match the tangential magnetic fields from both sides of the gap, $H_\phi(a+, z) = H_\phi(a-, z)$. This gives an integral equation which we propose to set up, in order to extract from it the performance data of the gap coupler as a plasma heating device.

Using Fourier analysis in axial direction and the radial wave functions defined by Eqs.(4), (5), and (7.1) we obtain the following field distribution valid throughout the plasma region:

$$E_z(r,z) = \frac{1}{2\pi}\int dk\, \frac{X_1(\lambda,\rho)}{X_1(\lambda,\alpha)}\, \hat{E}(k)\, e^{-jkz}$$

$$\left(\frac{\mu_o}{\epsilon_o}\right)^{1/2} H_z(r,z) = \frac{1}{2\pi}\int dk\, \frac{X_2(\lambda,\rho)}{X_1(\lambda,\alpha)} \left(-jk\frac{c}{\omega}\right) \hat{E}(k)\, e^{-jkz}$$

$$= \frac{c}{2\pi\omega}\frac{\partial}{\partial z}\int dk\, \frac{X_2(\lambda,\rho)}{X_1(\lambda,\alpha)}\, \hat{E}(k)\, e^{-jkz} \qquad (13)$$

$$E_\phi(r,z) = \frac{-jc}{2\pi\omega}\frac{\partial}{\partial z}\int dk\, \frac{X_3(\lambda,\rho)}{X_1(\lambda,\alpha)}\, \hat{E}(k)\, e^{-jkz}$$

$$\left(\frac{\mu_o}{\epsilon_o}\right)^{1/2} H_\phi(r,z) = \frac{j}{2\pi}\int dk\, \frac{X_4(\lambda,\rho)}{\rho X_1(\lambda,\alpha)}\, \hat{E}(k)\, e^{-jkz}$$

$$E_r(r,z) = \frac{-c}{2\pi\omega}\frac{\partial}{\partial z}\int dk\, \frac{\epsilon_x X_3(\lambda,\rho) + X_4(\lambda,\rho)}{\rho\,\epsilon_\perp X_1(\lambda,\alpha)}\, \hat{E}(k)\, e^{-jkz}$$

$$\left(\frac{\mu_o}{\epsilon_o}\right)^{1/2} H_r(r,z) = \frac{1}{2\pi}\int dk\, \frac{\lambda X_3(\lambda,\rho)}{\rho X_1(\lambda,\alpha)}\, \hat{E}(k)\, e^{-jkz}$$

Note that we have replaced any odd factor k in the integrand by differentiation with respect to z. This trick helps to keep track of the proper signs arising in the final answer for waves which travel in opposit direction. Our ansatz evidently matches the prescribed field distribution $E_z(a,z) = E(z)$, as well as the boundary condition $E_\varphi(a,z) = o$, which is satisfied identically by the very definition of $X_3(\lambda, \varrho)$ in Eq.(7.1). We now introduce the Green's function

$$\underline{\mathcal{G}}(r,z) = \frac{1}{2\pi}\int_{-\infty}^{+\infty} \frac{\underline{X}(\lambda,\varrho)}{X_1(\lambda,\varrho)} e^{-jkz}\, dk$$

$$= -\frac{j\omega}{2c} \sum_{n=1}^{\infty} \frac{\underline{X}_n(\varrho)}{X_{1,\lambda n}(\alpha)\, K_n} e^{-jk_n|z|} \qquad (14.1)$$

which we have evaluated by residue calculation at the poles $\pm k_n$, Eq.(7.3), of the integrand. In this context it was necessary to remember that the steady state, $\omega = \omega_r$, is obtained from Laplace analysis in the limit, $\omega = \omega_r - j|\varepsilon|$, $|\varepsilon| \to o$, so that the poles $\pm k_n$ are moved slightly off the real k axis as shown in Fig.5. This procedure works also in the perfectly loss free case. Now the displaced contours of integration shown in Fig.5 are uniquely determined by the convergence of the exponential factor, exp(-jkz), in the integrand. By taking the residues in the sens indicated, one recovers the result stated in Eq.(14.1).We now introduce the normalized eigenfunctions, Eq.(9.6), then the wave impedance as defined in Eq.(11.3), which gives

$$\frac{\underline{X}_n(\varrho)}{X_{1,\lambda_n}(\alpha)} = \underline{R}_n(\varrho)\, R_{4n}(\alpha) = \underline{R}_n(\varrho)\, \frac{1}{\sqrt{2\pi}} \left(\frac{\mu_o}{\epsilon_o}\right)^{1/4} \left(\frac{K_n}{Z_n}\right)^{1/2},$$

and brings the Green's function Eq.(14.1) into the form

$$\underline{\mathcal{G}}(r,|z|) = \sum_{n=1}^{\infty} \underline{\mathcal{X}}_n(\varrho)\, \frac{-e^{-jk_n|z|}}{2\sqrt{Z_n}} \qquad (14.2)$$

where the radial wave function

$$\underline{\mathcal{X}}_n(\varrho) \equiv \frac{j\omega/c}{\sqrt{2\pi}} \left(\frac{\mu_0}{\epsilon_0}\right)^{1/4} K_n^{-1/2}\, \underline{R}_n(\varrho) \tag{14.3}$$

has been introduced as a short-hand notation. In applying the theorem of convolution to the Eqs.(13),

$$\frac{1}{2\pi}\int \hat{\underline{\mathcal{G}}}(r,k)\,\hat{E}(k)\,e^{-jkz}\,dk = \int \underline{\mathcal{G}}(r,|z-\zeta|)\,E(\zeta)\,d\zeta \quad ,$$

we are led to define the amplitude factor

$$U_n(z) \equiv -\frac{1}{2\sqrt{Z_n}} \int_{-\infty}^{+\infty} e^{-jk_n|z-\zeta|}\,E(\zeta)\,d\zeta \quad [VA]^{1/2} \tag{15}$$

and obtain the electromagnetic field components in their final form:

$$\begin{aligned}
E_z(r,z) &= \sum_{n=1}^{\infty} \mathcal{X}_{1n}(\varrho)\,U_n(z) \\
H_z(r,z) &= \left(\frac{\epsilon_0}{\mu_0}\right)^{1/2} \sum_{n=1}^{\infty} \mathcal{X}_{2n}(\varrho)\,\frac{c}{\omega}\,\frac{\partial}{\partial z}\,U_n(z) \\
E_\phi(r,z) &= -j \sum_{n=1}^{\infty} \frac{1}{\varrho}\,\mathcal{X}_{3n}(\varrho)\,\frac{c}{\omega}\,\frac{\partial}{\partial z}\,U_n(z) \\
H_\phi(r,z) &= j\sqrt{\frac{\epsilon_0}{\mu_0}} \sum_{n=1}^{\infty} \frac{1}{\varrho}\,\mathcal{X}_{4n}(\varrho)\,U_n(z) \\
E_r(r,z) &= -\sum_{n=1}^{\infty} \frac{1}{\varrho\epsilon_\perp}\left[\epsilon_x \mathcal{X}_{3n}(\varrho) + \mathcal{X}_{4n}(\varrho)\right]\frac{c}{\omega}\,\frac{\partial}{\partial z}\,U_n(z) \\
H_r(a,z) &= \sqrt{\frac{\epsilon_0}{\mu_0}} \sum_{n=1}^{\infty} \frac{1}{\varrho}\,\lambda_n \mathcal{X}_{3n}(\varrho)\,U_n(z)
\end{aligned} \tag{16}$$

This solution would be complete, where it not for the electric field in the gap, E(z), which we do not know. To find it we must solve Maxwell's equations for $r \geqq a$, a job we would like to leave up to the microwave engineer. However, we can anticipate his answer, which has the form

$$H_\phi(a+,z) = \int_{-d/2}^{+d/2} \mathcal{G}^+(z,\zeta)\, E(\zeta)\, d\zeta \tag{17.1}$$

where $\mathcal{G}^+(z,\zeta) = \mathcal{G}^+(\zeta,z)$ is a symmetric Green's function, in general complex and therefore non hermitian like ours, $G(z,\zeta) = j(\varepsilon_o/\mu_o)^{1/2} G_4(a-, |z-\zeta|)$. Matching his magnetic field to ours, $H_\phi(a-,z)$, gives the required integral equation for the electric field, $E(z)$, in the gap

$$F(z) \equiv \int_{-d/2}^{+d/2} [\mathcal{G}^-(z,\zeta) - \mathcal{G}^+(z,\zeta)]\, E(\zeta)\, d\zeta = 0 \tag{17.2}$$

We now use an argument due to J. Schwinger[8] which dispenses us, under certain conditions, from the job of actually finding solutions of this integral equation. The argument is based on the fact that we are interested in the power flow across the gap, rather than in the electric field itself. In other words, if we could get a good match of the admittances looking both ways through the gap, we could not care less, if that was obtained with a not so good solution of the integral equation, Eq.(17.2). To define these admittances we use Poynting's theorem

$$2P^*_{+r} = -2\pi a \int_{-d/2}^{+d/2} E^*(z)\, H_\phi(a+,z)\, dz = e^*\, i_+ = e^* e\, Y_{+r}(\omega) \tag{18.1}$$

$$2P^*_{-r} = 2\pi a \int_{-d/2}^{+d/2} E^*(z)\, H_\phi(a-,z)\, dz = e^*\, i_- = e^* e\, Y_{-r}(\omega)\,, \tag{18.2}$$

and an r.f. potential, e [Volt], such that

$$e = -\int_{-d/2}^{+d/2} E(z)\,dz\,, \qquad E(z) = -e\,g(z)\,, \qquad g(z) = 0 \;\; |z| > \frac{d}{2} \tag{18.3}$$

The gap-factor g(z) [cm^{-1}], introduced here can be looked upon as the field distribution due to an r.f. potential of 1 volt across the gap. The application of Schwinger's argument then proceeds as follows. A perfect match would require a gap factor, g(z), such that the sum of the two admittances, i.e.

$$Y = Y_{+r} + Y_{-r} = \iint g^*(z)\,\mathcal{G}(z,\zeta)\,g(\zeta)\,dz\,d\zeta$$

vanishes. Note $\mathcal{G} \equiv \mathcal{G}^- - \mathcal{G}^+$. Now consider a gap factor $g_o(z)$ with deviation $\delta g(z) = g_o(z) - g(z)$ from the exact one. That results into a mismatch,

$$\delta Y = \iint \delta g^*(z)\,\mathcal{G}(z,\zeta)\,g(\zeta)\,dz\,d\zeta + \iint g^*(z)\,\mathcal{G}(z,\zeta)\,\delta g(\zeta)\,dz\,d\zeta\,,$$

the first term of which vanishes because, g = E/e is a solution of Eq.(17.2), while the last one does not, unless the Green's function is hermitian $\mathcal{G}(\zeta, z) = \mathcal{G}(z,\zeta)^*$, or g(z) is real. The first condition can not be met in our case. However, the last condition is satisfied when the fields in the gap region itself behave quasistationary, an assumption we are certainly entitled to make. Thus, instead of solving Eq.(19) rigorously, we can guess a trial field which, when fairly close to the correct form, g(z), will give only errors of the second order in calculations of the power flow. For example we can use the "gap factor"

$$g(z) = \frac{1}{\sqrt{\pi}}\,\frac{2}{d}\,\frac{\Gamma(1+\nu)}{\Gamma(\frac{1}{2}+\nu)}\,\left[1 - (2z/d)^2\right]^{\nu-1/2} \tag{19.1}$$

obtained by conformal mapping of the electrostatic field in the vicinity of coners with angle $\Theta = 4\pi\,\nu/(1+2\nu)$. We also state here its Fourier transform, commonly called "gap-modulation factor" in microwave tube engineering,

$$\hat{g}(k) = \Gamma(1+\nu)\, J_\nu(kd/2)\,(kd/4)^{-\nu} \tag{19.2}$$

as well as the transform of the "gap-correlation factor"

$$G(z) \equiv \int g(\zeta)\, g(\zeta+z)\, d\zeta \quad \longrightarrow \quad \hat{G}(k) = \hat{g}(k)\,\hat{g}(-k), \tag{19.3}$$

and its Hilbert transform:

$$\hat{H}(k) \equiv \frac{1}{\pi} \int \frac{\hat{G}(k')}{k'-k}\, dk' = -\frac{2^{2\nu+1}\,\Gamma^3(1+\nu)}{\pi\,\Gamma(\nu+\tfrac{3}{2})\,\Gamma(2\nu+\tfrac{3}{2})} \cdot$$

$$\frac{kd}{2}\; {}_2F_3\left[1,\, 1+\nu;\; \tfrac{3}{2},\, \tfrac{3}{2}+\nu,\, \tfrac{3}{2}+2\nu;\; -\left(\tfrac{kd}{2}\right)^2\right] \tag{19.4}$$

We are now ready to evaluate the performance of the gap coupler. Starting with the surface current,

$$i' = -2\pi a\, H_\phi(a, z) = \sum_{n=1}^{\infty} u_n(z)/\sqrt{Z_n}\,, \tag{20.1}$$

obtained from Eqs.(16.4) and (11.3), we calculate the amplitude factor, Eq.(15), in its explicite form

$$u_n(z) = \frac{e}{2\sqrt{Z_n}} \int_{-\infty}^{+\infty} e^{-j k_n |z-\zeta|}\, g(\zeta)\, d\zeta \tag{20.2}$$

$$= \frac{e}{2\sqrt{Z_n}}\, \hat{g}(k_n)\, e^{-j k_n z} \equiv u_n^+(z)\,, \quad z > \frac{d}{2} \tag{20.3}$$

$$= \frac{e}{2\sqrt{Z_n}}\, \hat{g}(-k_n)\, e^{j k_n z} \equiv u_n^-(z)\,, \quad z < -\frac{d}{2} \tag{20.4}$$

We then can estimate the losses in the pipe containing the plasma as follows

$$L = \frac{1}{2} R_s \sum_{n=1}^{\infty} 2 \cdot \int_{d/2}^{\ell/2} i_n i_n^* \, dz = \frac{1}{2} R_s \sum_{n=1}^{\infty} \int_{d/2}^{\ell/2} \left| \frac{U_n^+}{\sqrt{Z_n}} \right|^2 dz$$

$$\approx \frac{1}{2} R_s \sum_{n=1}^{\infty} \left| \frac{U_n^+(0)}{\sqrt{Z_n}} \right|^2 \frac{e^{-|\mathrm{Im}\, k_n| d} - e^{-|\mathrm{Im}\, k_n| \ell}}{|\mathrm{Im}\, k_n|} \rightarrow \frac{1}{2} \sum_{n=1}^{\infty} \frac{R_s}{|\mathrm{Im}\, k_n|} \left| \frac{U_n^+(d/2)}{\sqrt{Z_n}} \right| \qquad (20.5)$$

where, R_s = Real $(j\omega/u_o/\sigma)^{1/2}$, is the conventional surface resistance due to the skin depth penetration of the waves into the metal, and "ℓ" the length of the system. Note that the last step, $\ell \rightarrow \infty$, is not permissible in a loss free plasma where Im $k_n = o$. It is obvious from these formulae that the wall losses decrease as the losses in the plasma increase!

Next we calculate the admittance Eq.(18.2) of the plasma as seen through the gap. The H_ϕ-component in that expression has already been calculated in general terms, Eq.(2o.1), so that we have

$$Y_r = \frac{1}{e} \sum_{n=1}^{\infty} \frac{1}{\sqrt{Z_n}} \int g^*(z) U_n(z) \, dz \,, \qquad (21.1)$$

and when U_n assumes the special form, Eqs.(2o.2), we get

$$Y_r = \sum_{n=1}^{\infty} \frac{1}{2 Z_n} \iint dz\, d\zeta \; g(z) g(\zeta) \, e^{-j k_n |z-\zeta|} \qquad (21.2)$$

The substitution $Z = \zeta - x$ produces the gap correlation factor already defined in Eq.(19.3), then

$$Y_{-r} = \sum_{n=1}^{\infty} \frac{1}{2Z_n} \int_{-\infty}^{+\infty} dx\, G(x)\, e^{-jk_n|x|} = \frac{1}{2Z_n}\left[\int_{-\infty}^{0} dx\, G(x)\, e^{jk_n x} + \int_{0}^{\infty} dx\, G(x)\, e^{-jk_n x}\right]$$

$$= \sum_{n=1}^{\infty} \frac{1}{2Z_n}\left[\hat{G}_{-}(k_n) + \hat{G}_{+}(-k_n)\right] \qquad (21.3)$$

where the "Laplace transforms" $\hat{G}_{\pm}$ of G(x) are identical with the positive and negative "frequency parts" of $\hat{G}(k)$:

$$\hat{G}_{\pm}(k) = \frac{1}{2}\left[\hat{G}(k) \mp j\hat{H}(k)\right] \qquad (21.4)$$

Because $\hat{G}(k)$ is an even function of k, its Hilbert transform $\hat{H}(k)$ is odd, so that we obtain the final result

$$Y_{-r}(\omega) = \frac{1}{2} \sum_{n=1}^{\infty} \left[\hat{G}(k_n) + j\hat{H}(k_n)\right] / Z_n \qquad (21.5)$$

To uncover the physical contents of this formula, we remember that $\hat{G}(k) = \hat{g}(k)\hat{g}(-k)$, Eq.(19.3), and introduce from Eq.(2o.2) and Eq. (2o.3) the wave amplitudes, $U_n^{\pm}(o)/e$, referred back to the midplane of the gap. The resulting expression

$$Y_{-r}(\omega) = \sum_{n=1}^{\infty}\left[2\,\frac{U_n^{+}(o)}{e}\,\frac{U_n^{-}(o)}{e} + j\hat{H}(k_n)/2Z_n\right]$$

clearly identifies the real part of the gap admittance as an inverse "radiation resistance" due to the excited plasma waves. Thus the total R.F. power injected into the device is given by

$$P = \text{Real}\ \frac{1}{2} e i^{*} = \text{Real}\ \frac{1}{2} e e^{*} Y_{-r}(\omega) \qquad (21.6)$$

and the plasma heating efficiency can now be calculated from

$$\eta = 100\,(1 - L/P)\ \% \qquad (21.7)$$

In Fig.6 we show a sample calculation of the gap impedance $Z(\omega) = 1/Y_{-r}(\omega)$ due to a spectrum of the electromagnetic Trievelpiece-Gould waves of Fig.1. Its real part, i.e. the "radiation resistance", smoothly follows the trend of the wave impedance shown earlier in Fig.2. This is due to a proper choice, $|k_n d| \ll 2\pi$, of the gap width, which enters the calculation via the gap-modulation factor: Eq.(19.2) with $\nu = 1/2$ in this graph. Obviously the condition $|k_n d| \ll 2\pi$ can not be satisfied for all the higher order modes, and certainly not near the electron plasma frequency ω_{pe}, where $k_n \to \infty$. The gap modulation factor becomes oscillatory there, producing wiggles on the impedance characteristics. The onset of this phenomenon can be seen at the high frequency end of our graph. The reactive part of the gap-impedance is inductive and, compared with the real part, quite small. The latter is again due to a proper choice of the gap modulation factor, $|k_n d| \ll 2\pi$, as can be seen from an inspection of Eq.(19.4). The smooth variation with frequency of both, the resistive and reactive part of the gap impedance are a delight to the microwave engineer confronted with the job of matching the gap-coupler to an R.F. generator. This should be contrasted with the nightmare of matching a generator to resonant peaks in cavity absorption. To maintain the broad band characteristics of the gap coupler in such a system, for example, in a toroidal device, we must be sure that the plasma waves are absorbed before they get once around. If this can be obtained depends entirely on the damping, $\mathrm{Im}\, k_n$, which will be due to parametric decay of the waves, provided the frequency is high enough. Even if that scheme works in principle we are confronted with another difficulty which arises from the fact that it is well neigh impossible to feed 10 to 20 megawatts of power, as needed in R.F. heating of fusion plasmas, through a single parthole. We are thus confronted with the interaction of many coupling devices, the fundamentals of which will be discussed in the following chapter.

4. Slow-Wave Excitation of Plasma Waves

In the previous chapter we solved inhomogeneous boundary conditions at the wall of a plasma loaded waveguide, excluding reflexions from the ends. Thus, outside the gap region we were confronted only with propagating waves. If we want to study the interaction of many coupling devices, we also must allow for standing waves, in all the spaces inbetween. This is in particular true if we want to put the plasma waves to work by constructive interference with circuit waves, which necessarily must be coupled to the plasma in some space periodic fashion. In Fig.7 we show how such a wave-directional coupler may look like. It uses a Millman line fed from a tapered-ridge waveguide with a periodic array of slits to do the coupling with the plasma waves. The purpose of the Millman line is to match the speed of the circuit waves to that of the plasma waves for maximum energy transfer, as we shall see later. Although such a distributed coupling scheme may be the answer to many problems of power handling capabability in R.F. plasma heating, we are not yet in a position to predict the performance of a device of that complexity. As a first step in that direction we propose to treat a model with added symmetry, as shown in Fig.8. It uses a periodic array of gaps in a cylindrical plasma waveguide coupled to an iterated circuit, the specifications of which are dictated by the plasma waves supposed to do the heating. It is the objective of this chapter to supply a general formalism by which the missing specifications can be obtained, using the model of Fig.8 as a guidline.

As a first step towards a book keeping of the injected and reflected waves between the gaps in Fig.8, let us specify surface currents left and right from a selected gap, say

$$\begin{aligned} i(z) &\rightarrow i^{(1)} \quad \text{at} \quad z = -\ell_1 \\ i(z) &\rightarrow i^{(2)} \quad \text{at} \quad z = \ell_2 \end{aligned} \tag{22}$$

Obviously, this "choice" must be made selfconsistent with the rest of the system, a task which is easily acomplished later when we

actually evaluate the performance of the system. To match the boundary conditions at these two "virtual terminals", we must add to the propagating waves of Eqs.(16), a spectrum of standing waves which satisfies the homogeneous boundary conditions of an unobstracted wall. Since these are proportional to the radial eigenfunctions, e.g. in the form $\underline{\chi}_n(\rho)$ of Eq.(14.3), all we have to do is to replace in Eqs.(16) the amplitude factor $U_n(z)$ defined in Eq.(15.) by

$$W_n(z) = a_n e^{-jk_n z} - b_n e^{jk_n z} + U_n(z) \qquad (23.1)$$

The modified surface currents $i_n(z)$ are then obtained from Eq.(2o.1) with W_n replacing U_n:

$$i_n(z) = W_n / \sqrt{Z_n} \qquad (23.2)$$

We must caution in this context, not to use Eq.(23.2) for calculating the power flow from Eq.(11.1), because that expression does not discriminate between power flowing to the left and right respectively. We therefore calculate the "mixed" Poynting-flux directly from Eqs.(16), using Eq.(1o.3), which give the remarkably simple result:

$$P_{np}(z) = \frac{1}{2} \frac{jW_n^*(z)}{|k_n|} \frac{\partial}{\partial z} W_p(z) \delta_{np} \qquad (24.1)$$

Due to the orthogonality of this expression we can treat from now on each mode individually:

$$P_n(z) = \frac{1}{2} \frac{jW_n^*(z)}{|k_n|} \frac{\partial}{\partial z} W_n(z) \equiv \frac{1}{2} i_n^*(z) e_n(z) = \frac{W_n^*(z)}{\sqrt{Z_n^*}} e_n(z) \qquad (24.2)$$

We have substituted the surface current Eq.(23.2) into this expression in order to define the r.f. plasma potential $e_n(z)$. A comparison of the second and last term in this expression gives

$$e_n(z) = \frac{j\sqrt{Z_n^*}}{|k_n|}\frac{\partial}{\partial z}W_n = j\left(\frac{Z_n^*}{k_n^* k_n}\right)^{1/2}\frac{\partial}{\partial z}W_n = \frac{j\sqrt{Z_n}}{k_n}\frac{\partial}{\partial z}W_n \,, \qquad (25.1)$$

where the last step is justified in Eq.(11.4).When we write Eqs. (23), and Eq.(25.1) in their explicite form

$$e_n(z) = \sqrt{Z_n}\,\frac{j}{k_n}\frac{\partial}{\partial z}W_n = \left[a_n e^{-jk_n z} + b_n e^{jk_n z} + \frac{j}{k_n}\frac{\partial}{\partial z}U_n(z)\right]\sqrt{Z_n} \qquad (25.2)$$

$$i_n(z) = W_n(z)/\sqrt{Z_n} = \left[a_n e^{-jk_n z} - b_n e^{jk_n z} + U_n(z)\right]/\sqrt{Z_n}, \qquad (25.3)$$

we see that the plasma mode potentials e_n, and associated surface currents i_n are uniquely determined by the wave amplitudes, a_n, b_n, U_n, and vica-versa. This set of equations therefore serves the same purpose as in microwave engineering, where it is used to balance the "incident" waves, a_n, and "reflected" waves, b_n, looking into a given terminal, for obtaining voltage-current relationships, compare e.g. Montgomery, Dicke and Purcell.[73] Our contribution $U_n(z)$ in Eqs.(25) allows in addition a distributed source or sink of power, which is properly balanced by Eqs.(24). These equations can therefore be looked upon as an extended Microwave Power Theorem. We shall now give a demonstration of the great advantages which can be drawn from this theorem in matching the boundary conditions at the "virtual terminals" proposed above.

Starting with the region outside the gap $|z| > d/2$, we can use Eq. (2o.3) and Eq.(2o.4) for $U_n(z)$ to obtain

$$\frac{j}{k_n}\frac{\partial}{\partial z}U_n = \operatorname{sgn}(z)\,U_n(z) \,, \quad |z| > d/2$$

which puts Eqs.(25) into the form

$$e_n(z) = \sqrt{Z_n}\,[\,a_n e^{-jk_n z} + b_n e^{jk_n z} + \mathrm{sgn}(z)\,U_n(z)\,] \qquad (26.1)$$

$$i_n(z) = \frac{1}{\sqrt{Z_n}}\,[\,a_n e^{-jk_n z} - b_n e^{jk_n z} + U_n(z)\,] \qquad |z| > d/2 \qquad (26.2)$$

We now must evaluate the effect of the standing waves on the gap admittance. Equation (21.1) applies in this case with W_n replacing U_n, thus giving the modified gap admittance due to the n-th mode

$$y_n = \frac{1}{e\sqrt{Z_n}} \int g(z)\, W_n(z)\, dz \qquad (26.3)$$

When W_n is substituted herein from Eq.(23.1) we obtain the modified surface current injected by the gap:

$$i_n^{(3)} = y_n\, e^{(3)} = \frac{1}{\sqrt{Z_n}}\,[\,a_n \hat{g}(-k_n) - b_n \hat{g}(k_n)\,] \qquad + Y_n \cdot e^{(3)} \qquad (27.1)$$

where Y_n is the contribution of the n-th mode to the gap impedance as already given in Eq.(21.5). Also note that we have introduced the superscript (3) to distinguish the gap current and potentials from those at the virtual terminals. The latter can now be written down, using Eqs.(26), and Eqs.(2o), at $z = -l_1$, and l_2 respectively:

$$z = -l_1 \qquad e_n^{(1)}/\sqrt{Z_n} = a_n e^{jk_n l_1} + b_n e^{-jk_n l_1} - U_n^{(1)} \qquad (27.2)$$

$$i_n^{(1)}\sqrt{Z_n} = a_n e^{jk_n l_1} - b_n e^{-jk_n l_1} + U_n^{(1)} \qquad (27.3)$$

$$z = l_2 \qquad e_n^{(2)}/\sqrt{Z_n} = a_n e^{-jk_n l_2} + b_n e^{jk_n l_2} + U_n^{(2)} \qquad (27.4)$$

$$-i_n^{(2)}\sqrt{Z_n} = a_n e^{-jk_n\ell_2} - b_n e^{jk_n\ell_2} + U_n^{(2)} \qquad (27.5)$$

where the minus sign in front of $i_n^{(2)}$ takes care of the engineering convention of counting currents positive when looking into the terminal, and

$$U^{(1)} = \frac{e}{2\sqrt{Z_n}}\hat{g}(-k_n)e^{-jk_n\ell_1}, \qquad U^{(2)} = \frac{e}{2\sqrt{Z_n}}\hat{g}(k_n)e^{jk_n\ell_2}$$

We have thus obtained a set of 5 equations, Eqs.(27), for a total of 8 variables, namely the mode amplitudes a_n, b_n, 3 potentials $e_n^{(i)}$ and 3 currents $i_n^{(i)}$. We can therefore eliminate the wave amplitudes a_n, b_n to obtain 3 linear relations between the applied potentials and currents. The process of elimination is tedious but straight forward. We therefore give here immediately the resulting admittance matrix:

$$i_n^{(i)} = \sum_{j=1}^{3} Y_n^{(i,j)} e_n^{(j)} \qquad i = 1,2,3 \quad , \quad e_n^{(3)} \equiv e^{(3)} \qquad (28.1)$$

where

$$Y_n^{(1,1)} = Y_n^{(2,2)} = \cot g\, k_n(\ell_1+\ell_2)/jZ_n \qquad (28.2)$$

$$Y_n^{(1,2)} = Y_n^{(2,1)} = -\operatorname{cosec} k_n(\ell_1+\ell_2)/jZ_n \quad , \qquad (28.3)$$

describe the transmission of the n-th mode between the virtual terminals in an unobstructed pipe, while

$$Y_n^{(1,3)} = Y_n^{(3,1)} = \left[\hat{g}_c(k_n)\cos k_n\ell_2 + \hat{g}_s(k_n)\sin k_n\ell_2\right] / \sin k_n(\ell_1+\ell_2)jZ_n \qquad (28.4)$$

$$Y_n^{(2,3)} = Y_n^{(3,2)} = -\left[\hat{g}_c(k_n)\cos k_n\ell_1 - \hat{g}_s(k_n)\sin k_n\ell_1\right] / \sin k_n(\ell_1+\ell_2)jZ_n \qquad (28.5)$$

$$Y_n^{(3,3)} = -jZ_n Y_n^{(1,3)} Y_n^{(2,3)} \sin k_n(l_1+l_2) - \frac{1}{2jZ_n}\left[\hat{H}_c(k_n)+\hat{H}_s(k_n)\right] \quad , \qquad (28.6)$$

describe the excitation of that mode via the gap. We also note that g_c and g_s are cosine- and sine transformations comming from even- and odd-parts of the gap factor respectively, so that

$$\hat{g}(k) = \hat{g}_c(k) + j\hat{g}_s(k) \quad , \quad \hat{G}(k) = \hat{g}_c^2(k) + \hat{g}_s^2(k) \quad , \quad \hat{H}(k) = \hat{H}_c(k) + \hat{H}_s(k)$$

The physical interpretation of these formulae is as follows: Closing the gap, $e^{(3)} = o$, gives the transmission line Eqs.(12), already described in chapter 2. We now would like to recover the results of chapter 3. We run immediately into trouble in this task, because the admittances, Eqs.(28), are all purely reactive for real k_n, while the gap admittance, Eq.(21.5), of chapter 3 has a resistive part, even when k_n is real. How can we reconcile the two? Suppose there are small losses in the system, so that $-\mathrm{Im}k_n = \varepsilon_n > o$, and let us take the virtual terminals to infinity, $l_1 = l_2 = \infty$. In this process we express the trigonometric functions in Eqs.(28) in terms of cotg $k_n l$, and use the fact that cotg $k_n l = j$ for $l \to \infty$, however, small the loss ε_n may be. In that limit the Y matrix becomes diagonal with elements $y_n^{11} = Y_n^{22} = 1/Z_n$, and $Y_n^{33} = Y_n$, which in fact is the contribution of the n-th mode to the gap impedance we have obtained in chapter 3, Eq.(21.5). This demonstration indicates how important internal reflexions may affect the electrical characteristics and performance of a heating scheme, when the losses in the plasma are too small. Satisfied that our admittance matrix can answer quite subtile questions posed by theory, we go into the other extreme by giving a demonstration of its engineering value. For this purpose we define an aberration distance δ_n

$$\mathrm{tg}(k_n\delta_n) \equiv \hat{g}_s(k_n) / \hat{g}_c(k_n) \quad , \qquad (29.1)$$

which measures the odd part of the gap field, and therefore will be quite small in any symmetrical device. By means of this distance we can express the matrix elements Eq. (28.4) and Eq.(28.5) in the form

$$y_n^{(1,3)} = w_n \cos k_n(\ell_2 - \delta_n) / jZ_n \sin k_n(\ell_1 + \ell_2) \tag{29.2}$$

$$y_n^{(2,3)} = -w_n \cos k_n(\delta_1 + \delta_n) / jZ_n \sin k_n(\ell_1 + \ell_2) \tag{29.3}$$

$$w_n^2 \equiv \hat{g}_c^2(k_n) + \hat{g}_s^2(k_n) = \hat{G}(k_n) \tag{29.4}$$

Exactly the same matrix elements can be obtained by a straight forward engineering calculation of the circuit shown in Fig.9, provided we take $l_2 - \delta_n$, $l_1 + \delta_n$, for the sections of homogeneous transmission lines, w_n for the turn ratio of the input transformer, and

$$B_n \equiv \hat{H}(k_n)/2Z_n = [\hat{H}_c(k_n) + \hat{H}_s(k_n)]/2Z_n \tag{29.5}$$

for the shunt admittance across the input terminals. In microwave engineering such a device is known as a T-junction. With the interpretation of its elements given here, it describes the exitation, propagation and damping of the n-th mode in minute detail. We amplified that statement because the description is exact if we use a rigorous solution of the integral Eq.(17.2) rather than a trial solution $g(z)$ to calculate the various gap factors in Eqs.(29). We therefore shall refer henceforth to the device shown in Fig.9 as the mode-equivalent T_n-junction. As in conventional microwave engineering, it turns out to be the basic unit for analyzing a great variety of devices. A demonstration of this idea will now be given, using the example of the slow-wave directional coupler shown in Fig.8.

We start by taking identical T_n-junctions with $\ell_1 = \ell_2 = \ell/2$, each corresponding to a unit cell in Fig.8. We can join these T_n-junctions at the cross bars, and obtain the mode-equivalent chains shown in Fig.1o. Note that due to the orthogonality condition Eq.(24.1) there is no other way of doing this. As in any space periodic system, we now invoke Floquets theorem, which requires a uniform phase shift $\varkappa$ of all the physical quantities along the chain, e.g.

$$e_n^{(2)} = e_n^{(1)} e^{-j\alpha\ell} \quad , \quad i_n^{(2)} = -i_n^{(1)} e^{-j\alpha\ell} \tag{30.1}$$

By taking these relations into the circuit equations, Eqs.(28.1), we can calculate the admittance looking into any gap along the chain:

$$\frac{i_n^{(3)}}{e^{(3)}} = y_n^- = y_n^{(3,3)} - \frac{1}{2} \frac{(y_n^{(1,3)} + y_n^{(2,3)} e^{-j\alpha\ell})(y_n^{(1,3)} + y_n^{(2,3)} e^{j\alpha\ell})}{y_n^{(1,1)} + y_n^{(1,2)} \cos(\alpha\ell)} \tag{30.2}$$

When we express the admittance elements in terms of the gap factors, Eqs.(28), this equation assumes the simple form,

$$y_n^- = j \left[\frac{\hat{H}_n^-}{2Z_n^-} + \frac{\hat{G}_n^-}{Z_n^-} \frac{\sin k_n^- \ell}{\cos k_n^- \ell - \cos \alpha\ell} \right] , \tag{30.3}$$

where we have introduced the superscript minus to distinguish plasma quantities from circuit quantities, which now must be considered. In fact we can treat Maxwell's equations in vacuum after the model we used in this paper, with answers that formally look alike. We thus can construct mode equivalent chains of T-junctions for circuit waves which must yield a gap admittance similar in form to ours:

$$y_n^+ = j \left[\frac{\hat{H}_n^+}{2Z_n^+} + \frac{G_n^+}{Z_n^+} \frac{\sin k_n^+ \ell}{\cos k_n^+ \ell - \cos \alpha\ell} \right] \tag{30.4}$$

We now connect all the chains in parallel at their base terminals as indicated in Fig.1o. That amounts to matching the admittances

$$y^+ = \sum_{n=1}^{\infty} y_n^+ \quad , \quad y^- = \sum_{n=1}^{\infty} y_n^-$$

looking both ways through the gap. The resulting coupled mode equation

$$y^+ + y^- = \sum_{n=1}^{\infty} j\left\{ \frac{\hat{H}_n^+}{2Z_n^+} + \frac{\hat{G}_n^+}{Z_n^+} \frac{\sin k_n^+ \ell}{\cos k_n^+ \ell - \cos \varkappa \ell} + \frac{\hat{H}_n^-}{2Z_n^-} + \frac{\hat{G}_n^-}{Z_n^-} \frac{\sin k_n^- \ell}{\cos k_n^- \ell - \cos \varkappa \ell} \right\} = 0 \qquad (31.1)$$

finally determines Floquet's propagation constant as a function of frequency, $\varkappa(\omega)$. It is therefore a dispersion relation which determines the propagation of waves along the coupled structures. To get an overview of the solutions of Eq.(31.1), we observe that its lefthand side switches sign near resonance, $\cos \varkappa \ell \approx \cos k_n \ell$, while the other terms vary slowly as a function of frequency. Mode coupling thus occurs only where two denominators nearly vanish simultaneously, say where

$$\cos \varkappa \ell \approx \cos k_n^- \ell \approx \cos k_p^+ \ell$$

That nearly requires coincidence of two wavenumbers, one due to a plasma wave, and one due to a circuit wave or a space harmonic there of

$$\varkappa \approx k_n^-(\omega) \approx \pm k_p^+(\omega) + q\, 2\pi/\ell \quad , \quad q = \text{integer} \qquad (31.2)$$

The situation is illustrated in Fig.11, where we have plotted the respective wave numbers as a function of frequency. The requested coincidence evidently arises at the points of intersection of the two characteristics. To investigate the mode coupling near such a point, (ω^x, k^x), we apply the well known partial-fraction expansion,

$$\frac{\sin k_n \ell}{\cos k_n \ell - \cos \varkappa \ell} = \frac{1}{\ell} \sum_{m=-\infty}^{m=+\infty} \frac{1}{\varkappa - k_n - m 2\pi/\ell} - \frac{1}{\ell} \sum_{m=-\infty}^{+\infty} \frac{1}{\varkappa + k_n - m 2\pi/\ell} \quad , \qquad (31.3)$$

in Eq.(31.1), then compile all the non-resonant terms into one slowly varying function, $A(\omega, \varkappa)$, which brings Eq.(31.1) into the simple form:

$$A(\omega,\varkappa) \pm \frac{\hat{G}_p^+/Z_p^+\ell}{\varkappa-(\pm k_p^+ + q\,2\pi/\ell)} + \frac{\hat{G}_n^-/Z_n^-\ell}{\varkappa-k_n^-} = 0 \qquad (31.4)$$

This result is rigorous so far. We now take the vicinity of the resonance, Eq.(31.2), into account, by evaluating the slowly varying coefficients in Eq.(31.4) at the point of coincidence under consideration, viz.,

$$C^+ \equiv \frac{\hat{G}[k_p^+(\omega^x)]}{Z_p^+(\omega^x)\,A(\omega^x,k^x)}\,, \quad C^- \equiv \frac{\hat{G}[k_n^-(\omega^x)]}{Z_n^-(\omega^x)\,A(\omega^x,k^x)} \qquad (32.1)$$

Equation (31.4) then becomes a simple quadratic for Floquet's propagation constant with solutions

$$\varkappa = \left(\frac{\varkappa_1+\varkappa_2}{2}\right) \pm \sqrt{\left(\frac{\varkappa_1-\varkappa_2}{2}\right)^2 \pm C^+C^-/\ell^2}\,, \qquad (32.2)$$

where we have used the abbreviations,

$$\varkappa_1 = k_n^-(\omega) + C^-/\ell\,, \quad \varkappa_2 = \pm k_p^+(\omega) + q\,2\pi/\ell \pm C^+/\ell\,, \qquad (32.3)$$

and the $\pm$ signs in front of the square root are uncorrelated with the others. The interpretation of that result is as follows. The sum total of non-resonant terms, $A(\omega^x, k^x)$, in Eqs.(32.1) are usually quite large so that the coefficients $C^\pm$ are small. We therefore find Floquet's propagation constants, $\varkappa \approx \varkappa_1$, and $\varkappa \approx \varkappa_2$, shifted from these of the uncoupled modes by small amounts, C^-/ℓ and $\pm C^+/\ell$ respectively, except extremly close to resonance, where

$$\varkappa \approx \varkappa_1 + \frac{1}{\ell}\sqrt{\pm C^+C^-}\,, \quad \varkappa \approx \varkappa_1 - \frac{1}{\ell}\sqrt{\pm C^+C^-}$$

The nature of the coupling therefore depends on the sign under the square-root which, following Eq.(32.3), is positive in case of for-

ward wave interaction, and negativ in case of backward wave interaction. The latter gives complex values for $\varkappa\ell$ resulting into a range of evanescent waves, which have been studied extensively, among others by the author[14-17] in the general context of his wave stability criteria. Fortunately stability is not an issue here, although the frequency bands of evanescent waves are of some concern. Two such bands are clearly evident in Fig.11, around ka $\approx$ 6.8, and ka $\approx$ 7.7, respectively. We have greatly exaggerated the frequency shifts in that figure in order to clearly show the principles involved. The plasma wave dispersion has been taken over from Fig.1, while the dispersion characteristics of the circuit wave and space harmonics, Eq.(31.2) represents a sketch aimed at obtaining broadband interaction with the lowest order radial mode, $k_{on}(\omega)$, of the plasma waves. This is not quite an arbitrary procedure but a strict requirement in order to obtain maximum transfer of power from the circuit wave to the plasma wave. We can proof this statement without further elaborations, because we have established in Eq.(32.2) a one to one correspondence with the conventional microwave theory of directional couplers. We therefore can quote by comparison, e.g. with the results presented in the excellent book by W.H. Louisell,[18] that the maximum fraction of power transferred from the circuit wave to a codirectional plasma wave is given by

$$F_1 = \frac{1}{1+\Delta} \quad , \quad \Delta \equiv \frac{1}{4}\left(\varkappa_1\ell - \varkappa_2\ell\right)^2 / C^+C^- \, . \qquad (33.1)$$

That occurs at a distance

$$L = \frac{\pi}{2}\,\ell \,/\sqrt{C^+C^-} \qquad (33.2)$$

from the point of injection, where as an evanescent plasma wave only reaches that far, and feeds a fraction

$$F_2 = \frac{\sinh^2 \frac{\pi}{2}\sqrt{1-\Delta}}{\cosh^2 \frac{\pi}{2}\sqrt{1-\Delta} \; - \Delta} \qquad (33.3)$$

of the injected power back towards the input terminals. For a perfect match, $\Delta \approx o$, that may amount up to 84 % of the input power, which is clearly an undesirable feature. Fortunately the frequency

ranges of evanescent waves are usually very narrow band, so that one may be able to avoid them in practice. All we have to do then is to closely match the circuit's phase and group velocity to that of the desired plasma wave, in as wide as possible a frequency range, $\Delta \approx o$. That will make the transfer of power complete, $F_1 = 1$, in a distance L, so that the circuit can be interrupted there. We can calculate the required distance L from our formulae once the circuit is designed after the specifications worked out here. The resulting device is expected to distribute the impact of power over a considerable area, with a very frequency insensitive load impedance offered to the generator. Both aspects are of prime importance in view of the very high power levels needed eventaully in the business of igniting a fusion reactor.

Summary and Conclusions

It was one objective of this paper to give a demonstration of how the powerful analytic techniques of microwave electronics can be applied to basic plasma physics, in order to obtain the engineering data needed in R.F. plasma heating. This is exemplified by the gap impedance of chapter 3, and the synthesis of a slow-wave directional coupler in chapter 4. The latter is but one of the possible applications of the mode-equivalent T-junction we have introduced in chapter 4. We could use it for example as it stands to evaluate the performance of a phased array of oscillators connected to several adjacent gaps, a system which has been seriously proposed for R.F. plasma heating. An arrangement which has much more appeal to us consists of a periodic array of gaps fed by a distributed amplifier. It also could be evaluated right away by the techniques offered in this paper. The fact that we have restricted our sample calculations to the frequency range between the lower-hybrid frequency and the electron plasma frequency does not imply any restriction of our work to that range. In fact we can handle any hybrid layers in chapter 2, which gives the characterisitc wave impedance and dispersion characteristics. Thats all what is needed in the engineering formulae presented in the subsequent chapters. However, we do need an extension of the work presented in chapters 3 and 4 to cases with azimuthal variation, so that we can treat the coupling devices in a perfectly realistic fashion. In this task we will have to solve the tough problem of non-reciprocal propagation, which in itself can lead to an interesting device, namely a unidirectional coupler. Another extension of this work which is of extrem importance in R.F. plasma heating would be the inclusion of nonlinear processes. We are quite confident that the type of analysis presented in this paper offers a head start in that direction, because it is the parametric coupling of distributed circuits where it all started from in the first place.

Acknowledgment

The author herewith greatfully acknowledges the help of Dr. F. Leuterer in setting up the computer program for obtaining the normal modes, to Mrs. M. Walter for executing the program and finally to Mrs. C. Schmid for rushing the manuscript through.

This work was performed under the terms of the agreement on association between the Max-Planck-Institut für Plasmaphysik and EURATOM.

References

1 T.H. Stix: The Theory of Plasma Waves, McGraw Hill Book Co., Inc., N.Y., 1962, Chapter 5

2 H. Derfler: J. Appl. Phys. 38, 5oo5 - 5o13 (1967)

3 H. Derfler: Theory of Electron Beam Tubes with Periodic Structure, Thesis at the Swiss Federal Institute of Technology, Verlag Leeman, Zürich, Switzerland, 1954

4 H. Derfler: Zs. Angew. Math. Phys. IV, Fsc.2, pp. 1o4 - 114, Zürich (1955)

5 H. Derfler: Zs Angew. Math. Phys. VI, Fsc.3, pp. 19o - 2o6, Zürich (1955)

6 H. Derfler: "Plasma Waves in Finite Electron Beams and their Interaction with Electromagnetic Field Waves", Traveaux du Congres International "Tubes Hyperfrequences", Vol. I, pp. 326 - 336, Edition Chiron, Paris, 1958

7 H. Derfler and F. Leuterer: Plasma Physics 14, 473 - 497 (1972)

8 J. Schwinger and B.A. Lippmann: Phys. Rev. 79, 469 (195o)

9 G.D. Birkhoff and R.E. Langer: Proc. Amer. Acad. of Arts and Sciences, Vol. 58, pp. 51 - 128 (1923)

1o A.W. Trievelpiece and R. Gould: J. Appl. Phys. 3o, 1784 (1959)

11 R.E. Langer: Trans. Americ. Math. Soc. 46, 151 - 19o and 467 (1939)

12 H. Gamo: J. Phys. Soc. Japan, Vol. 8, No. 2, 176 - 182 (1953)

13 C.G. Montgomery, R.H. Dicke, E.M. Purcell: Principles of Microwave circuits, McGraw Hill Book Co . Inc., N.Y. 1948, p. 146 ff.

14 H. Derfler: in Proceedings of the Fifth International Conference on Ionization Phenomena in Gases (North Holland, Amsterdam 1961) Vol. 2, p. 1423; and details in Electron Devices Research, QSR No. 18 (Electronics Laboratories, Stanford University, 1961), pp. 17 - 4o

15 H. Derfler: in Proceedings of the Eight International Conference on Phenomena in Ionized Gases, Springer Verlag, Vienna, 1967, p. 294

16 H. Derfler: Phys. Lett. 24A, 763 (1967)

17 H. Derfler: Phys. Rev. A1, 1467 (197o)

18 W.H. Louisell: Coupled Mode and Parametric Electronics, John Wiley + Sons, Inc., N.Y., London, 196o, pp. 26 - 32

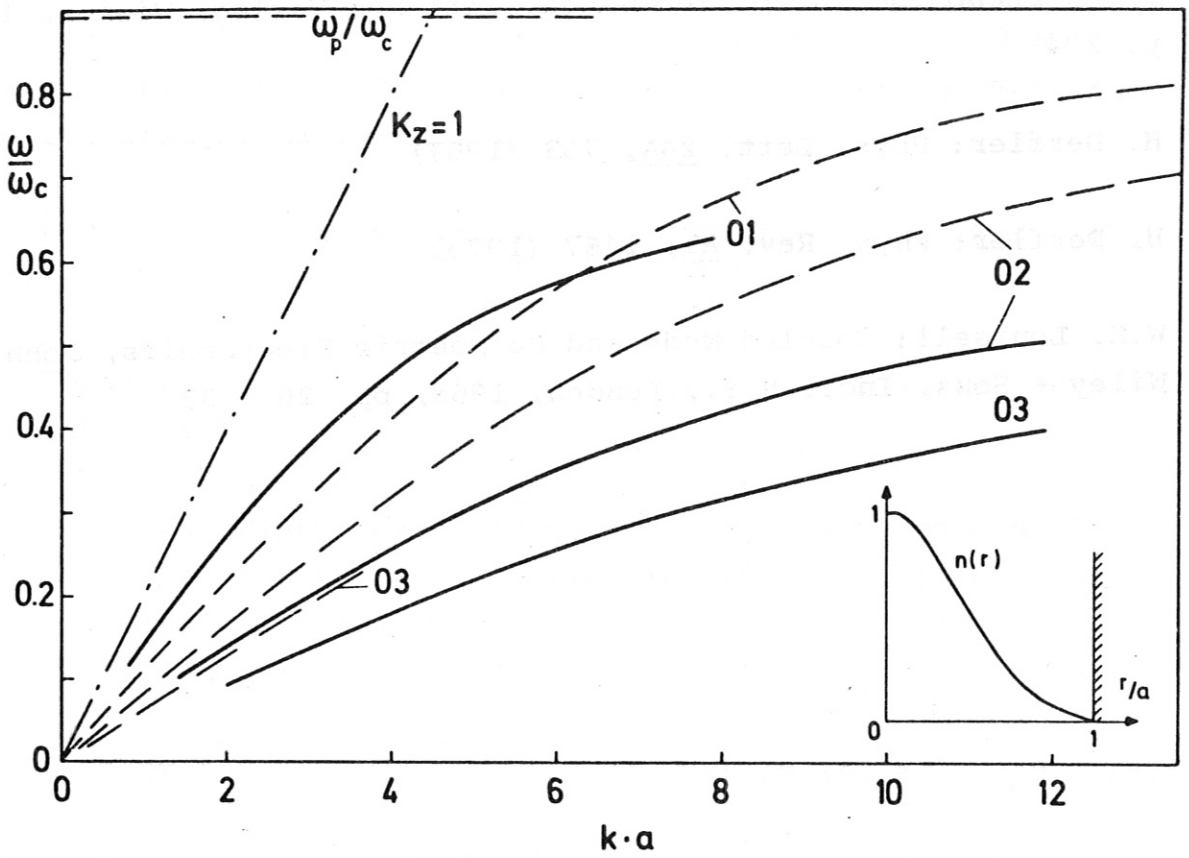

Fig.1 Electromagnetic wave dispersion in cylindircal waveguide filled with cold magneto plasma

Parameters: azimutal mode numbers m = o

radial mode numbers n = 1, 2, 3

$\omega_p^2(o)/\omega_c^2 = o.8$; $a\omega_c/c = 5$; $K_z = ck_z/\omega$

dashed lines: constant density

solid lines: Gaussian density profile

$n(r) = n(o) \cdot \exp - (2r/a)^2$

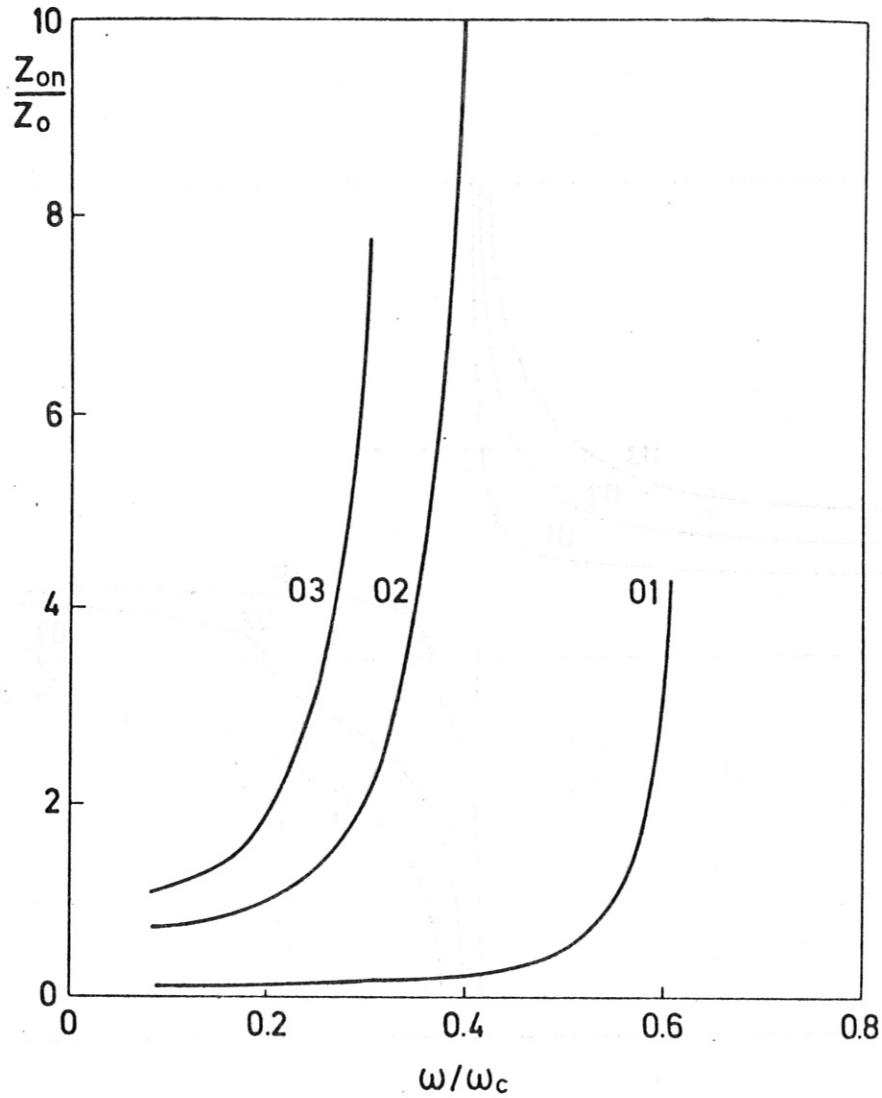

Fig.2 Characteristic mode impedance for radial modes in units of free-space impedance Z_o.
Parameters as in Fig.1, $Z_o = (\mu_o/\varepsilon_o)^{1/2} = 377$ Ohm

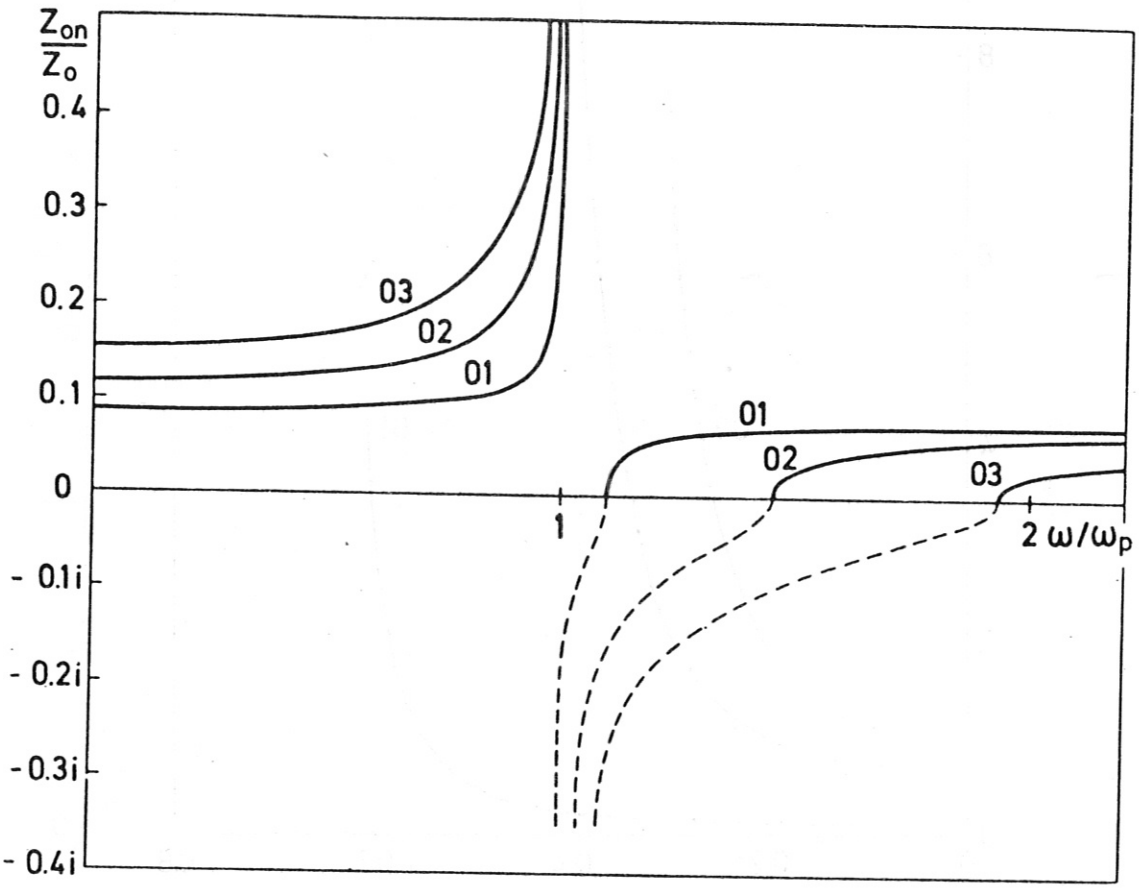

Fig.3 Characteristic wave impedance for radial modes in zylindrical plasma wave guide at infinite magnetic field.

Parameters: azimutal mode numbers m = o
radial mode numbers n = 1, 2, 3
cold plasma at constant density
$n = 2 \cdot 1o^{12}$ cm^{-3}, radius a = 2 cm

solid lines: resistive part of wave impedance
dashed lines: reactive part of wave impedance

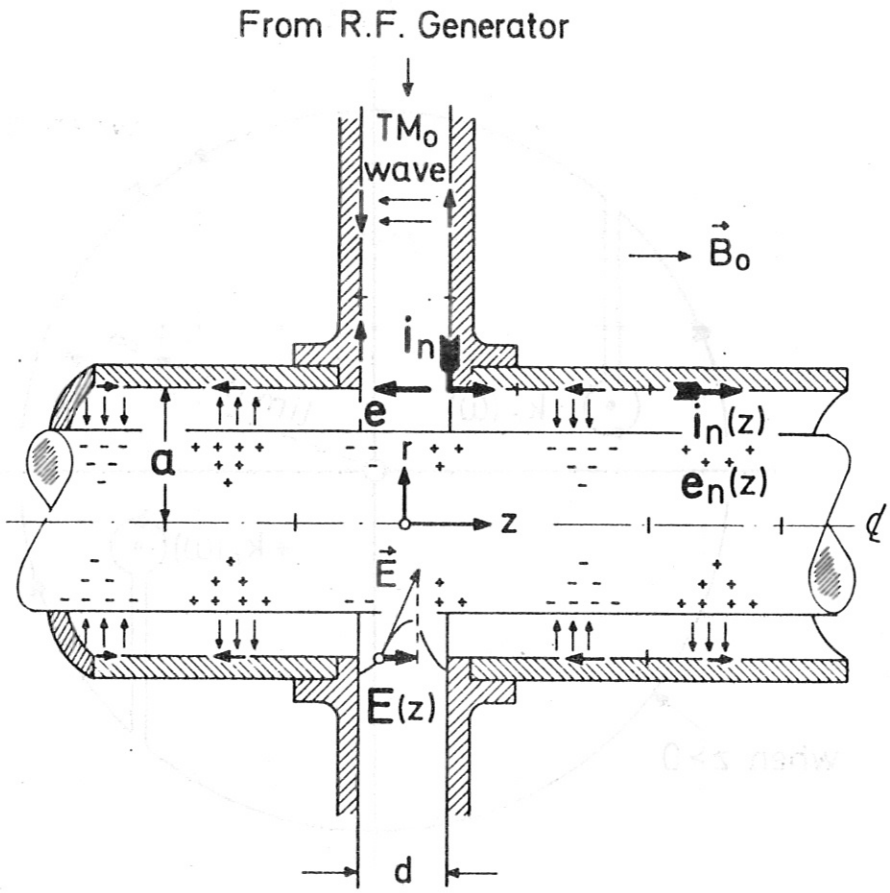

Fig.4 R.F. gap coupler

$E(z) = -eg(z)$ gap-field z-component

e = gap potential

i_n = gap current fed into n-th radial mode

$i_n(z)$ = surface current due to n-th mode

$e_n(z)$ = R.F. power equivalent "plasma potential" due to n-th radial mode

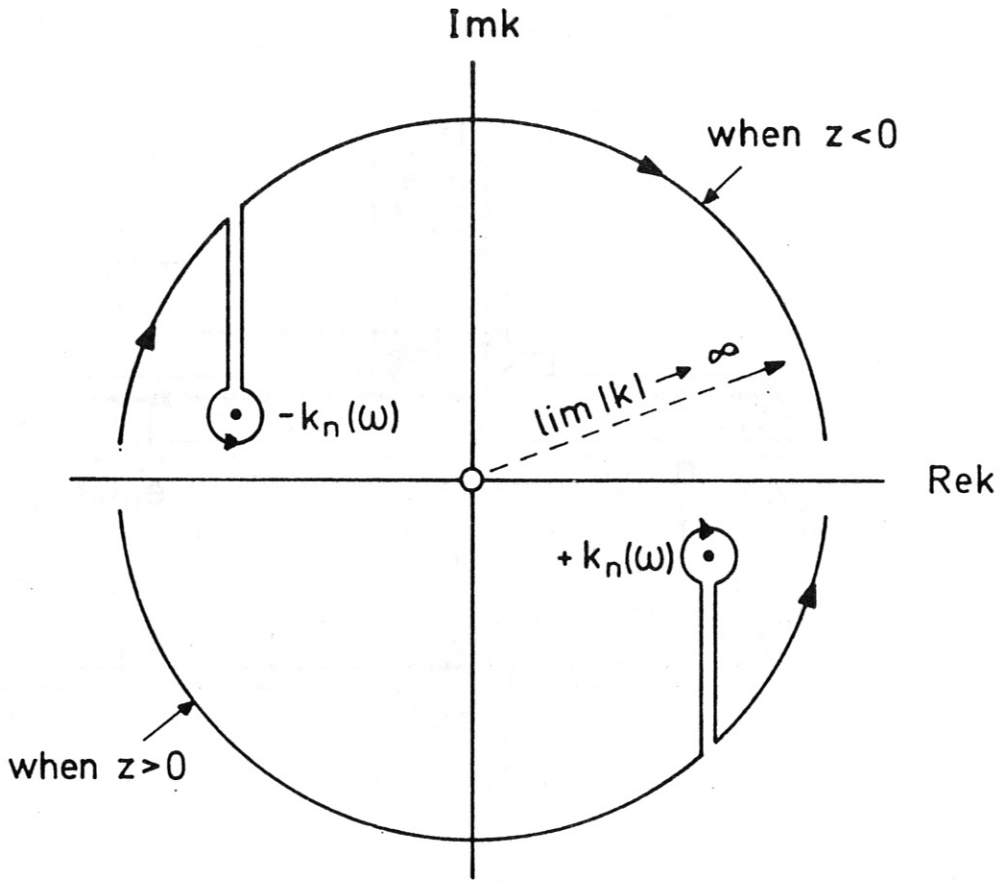

Fig.5 Complex wavenumber plane with displaced contours of integration used in residue calculation of Eq.(14.1)

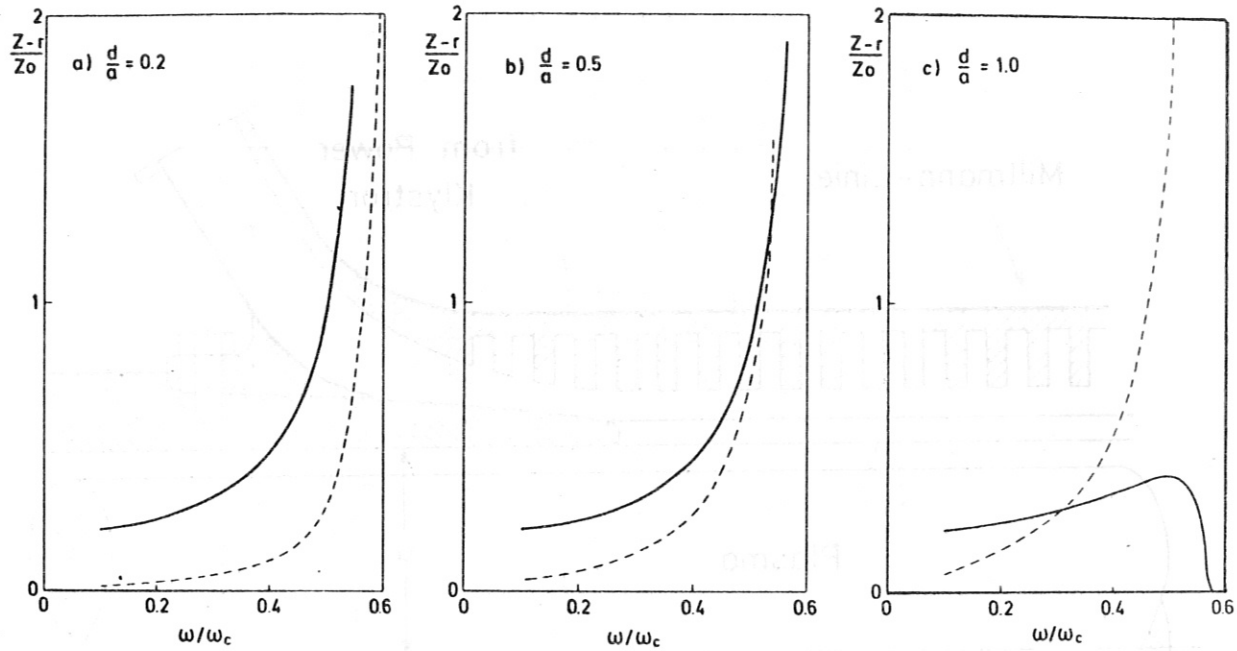

Fig.6 Gap-input impedance due to first three radial modes in zylindrical plasma waveguide, in units of free-space impedance, Z_o = 377 Ohm.
Gap width/radius = d/a: a) o.2, b) o.5, c) 1.o
Parameters as in Fig.1, with Gaussian density profile
solid line: resistive part of impedance
dashed line: reactive part of impedance

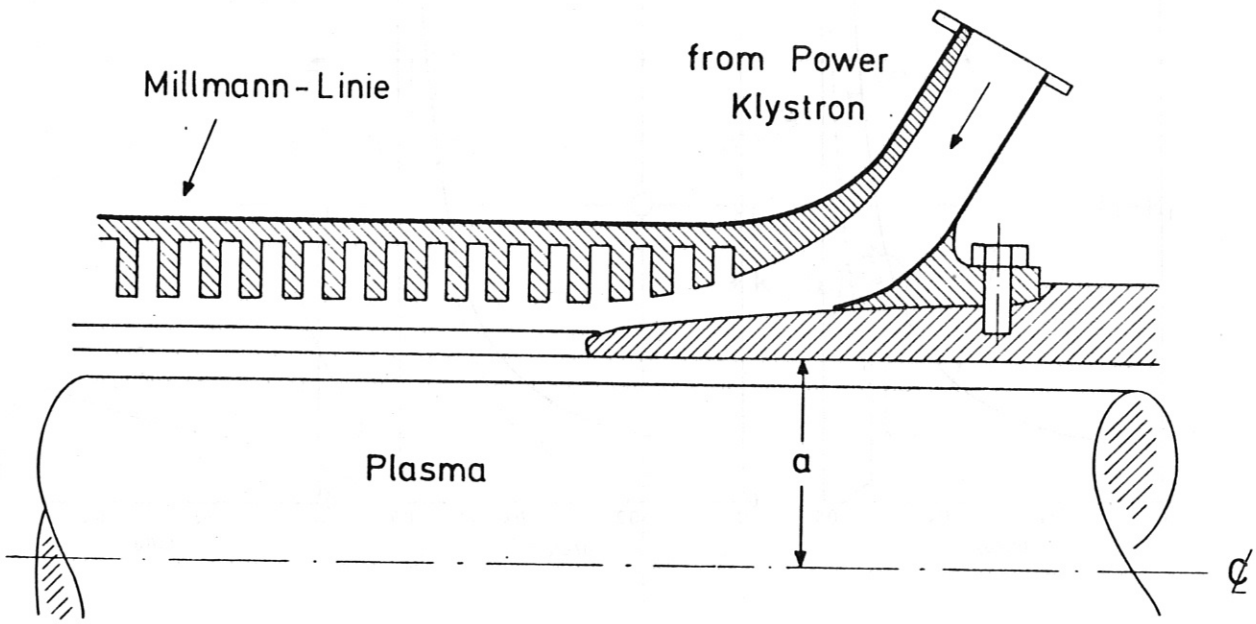

Fig.7 Sketch of proposed slow-wave directional coupler Millman-line delays electromagnetic wave to match phase and group velocity with these of a plasma wave for maximum power transfer in a broad frequency band.

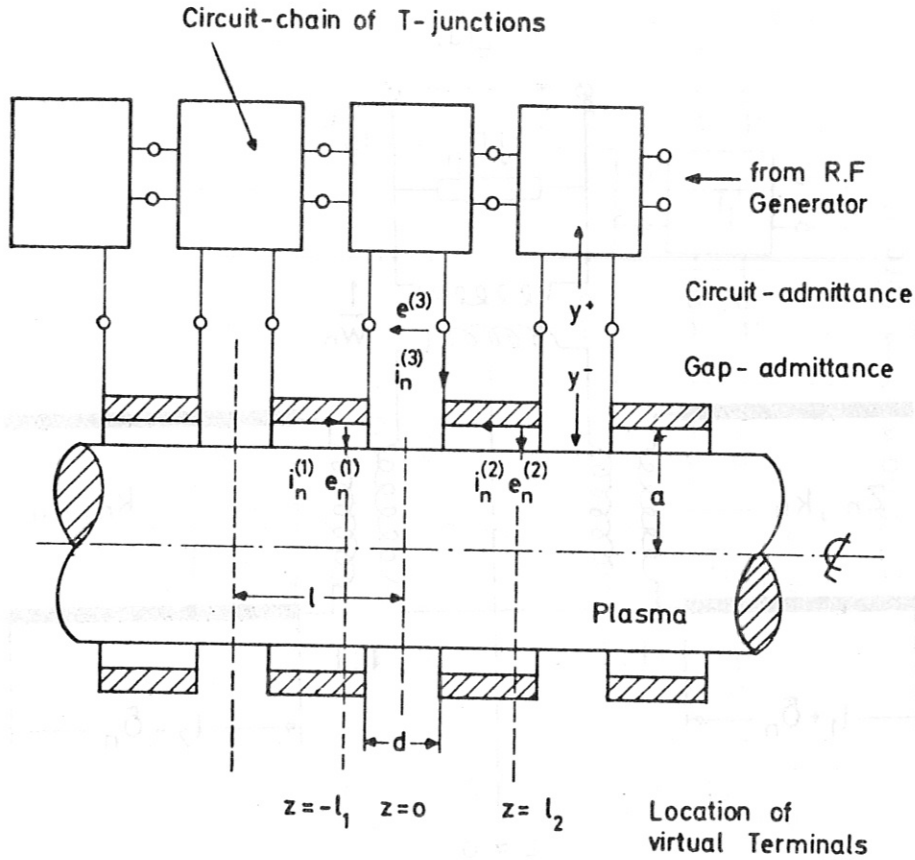

Fig.8 Coaxial model of slow-wave directional coupler. Chain of T-junction represents circuit analogue of delay line to match phase and group velocity of electromagnetic waves with that of plasma waves.

$i_n^{(i)}$ surface current of n-th mode

$e_n^{(i)}$ R.F. power-equivalent "plasma-potential" of n-th mode

Superscript (i), location of virtual terminal-pairs where quantity is measured.

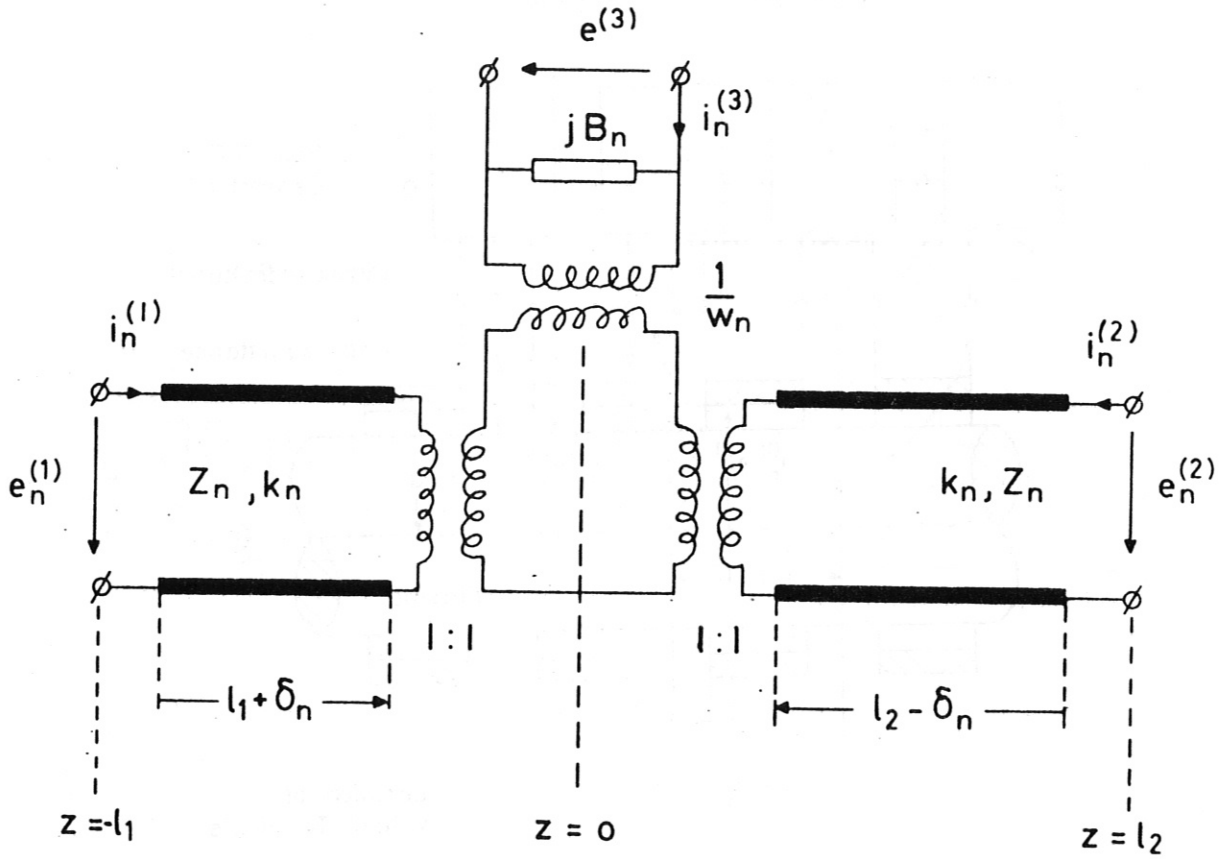

Fig.9 Mode-equivalent T_n-junction

w_n = turn ratio of input transformer = Square of Fourier transform of gap-field

B_n = input shunt admittance = Hilbert transform of w_n/ wave impedance Z_n

δ_n = aberration length vanishes in symmetrical devices

Circuit elements calculated in Eqs.(29)

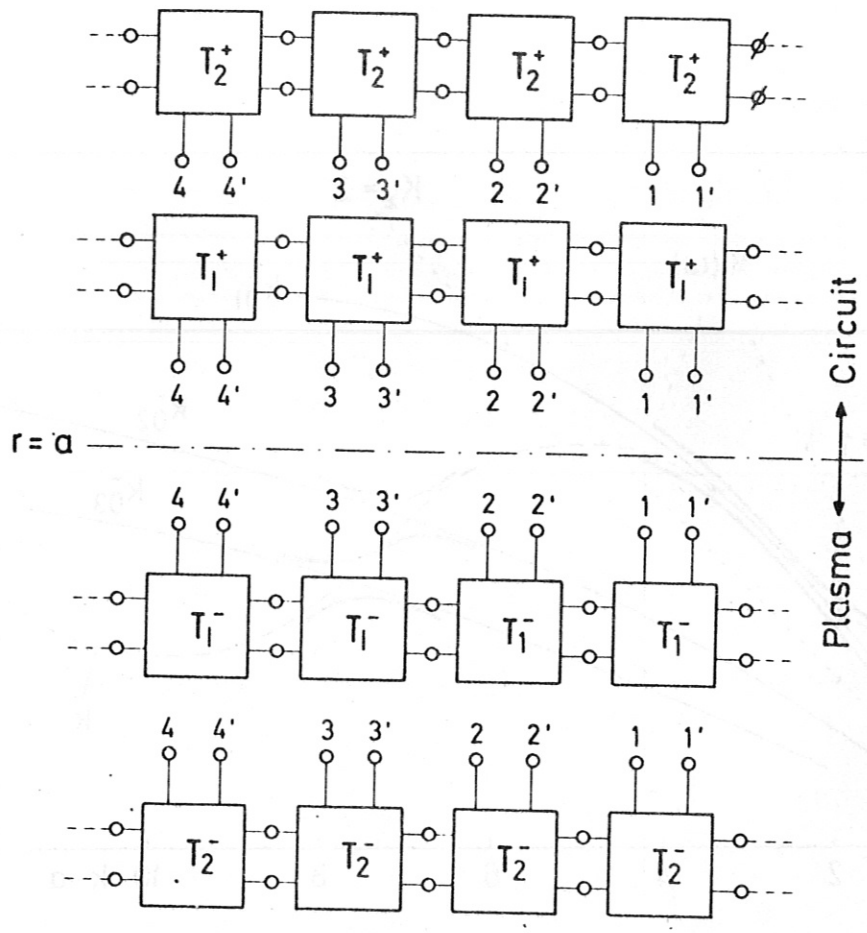

Fig.1o Chains of mode-equivalent T-junctions connected in parallel at the gap input terminals p p'

Superscript: + circuit waves
- plasma waves

subscript: n = mode number

In space-periodic structure, T_n-junctions are identical and chains are infinitly long or terminated by characteristic mode impedance Z_n: matched load or matched generator.

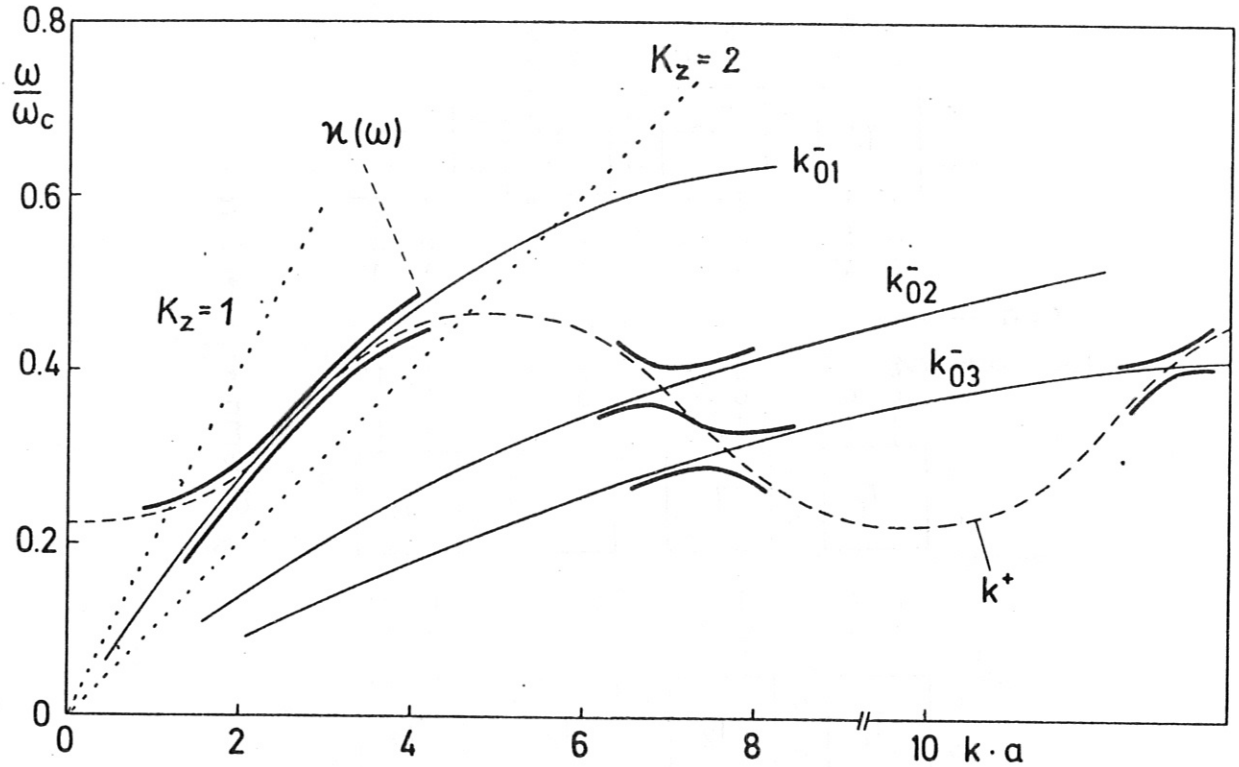

Fig.11 Dispersion characteristics of slow wave directional coupler to radial modes in a cylindrical plasma waveguide

thin line: dispersion of uncoupled radial plasma modes $\bar{k}_{on}(\omega)$, taken from Fig.1

dashed line: Dispersion of uncoupled circuit wave, $\ell/a \approx 0.7$ $o \leq k^{+}(\omega) \leq \pi/\ell$ and its first space harmonics $\pm k^{+}(\omega) + 2\pi/\ell$, schematically

thick line: Floquet's propagation constant of the coupled system, schematically